JOURNAL OF BACTERIOLOGY, May 2008, p. 3505–3525 Vol. 190, No. 10
0021-9193/08/$08.00+0 doi:10.1128/JB.01631-07

Effects of SecE Depletion on the Inner and Outer Membrane Proteomes of *Escherichia coli*▽†

Louise Baars,[1] Samuel Wagner,[1] David Wickström,[1] Mirjam Klepsch,[1] A. Jimmy Ytterberg,[2]‡ Klaas J. van Wijk,[2] and Jan-Willem de Gier[1]*

Center for Biomembrane Research, Department of Biochemistry and Biophysics, Stockholm University, SE-106 91 Stockholm, Sweden,[1] and Department of Plant Biology, Cornell University, 332 Emerson Hall, Ithaca, New York 14853[2]

Received 8 October 2007/Accepted 8 February 2008

The Sec translocon is a protein-conducting channel that allows polypeptides to be transferred across or integrated into a membrane. Although protein translocation and insertion in *Escherichia coli* have been studied using only a small set of specific model substrates, it is generally assumed that most secretory proteins and inner membrane proteins use the Sec translocon. Therefore, we have studied the role of the Sec translocon using subproteome analysis of cells depleted of the essential translocon component SecE. The steady-state proteomes and the proteome dynamics were evaluated using one- and two-dimensional gel analysis, followed by mass spectrometry-based protein identification and extensive immunoblotting. The analysis showed that upon SecE depletion (i) secretory proteins aggregated in the cytoplasm and the cytoplasmic σ^{32} stress response was induced, (ii) the accumulation of outer membrane proteins was reduced, with the exception of OmpA, Pal, and FadL, and (iii) the accumulation of a surprisingly large number of inner membrane proteins appeared to be unaffected or increased. These proteins lacked large translocated domains and/or consisted of only one or two transmembrane segments. Our study suggests that several secretory and inner membrane proteins can use Sec translocon-independent pathways or have superior access to the remaining Sec translocons present in SecE-depleted cells.

The genome of the gram-negative bacterium *Escherichia coli* harbors around 4,000 open reading frames (6, 9). Around 25% of these open reading frames encode inner membrane proteins, and around 10% encode secretory (i.e., periplasmic and outer membrane) proteins (17, 54). It is generally assumed that the Sec pathway is the major route for protein translocation across and insertion into the inner membrane of *E. coli* (37, 49). The targeting of secretory proteins to the Sec translocon is mostly posttranslational and can be facilitated by the cytoplasmic chaperone SecB (5, 19, 53). Inner membrane proteins are targeted to the Sec translocon via the signal recognition particle pathway in a cotranslational fashion (19, 37). In *E. coli*, a small number of proteins are translocated across or integrated into the inner membrane via the twin-arginine protein transport (TAT) pathway (28, 36, 61).

The core of the Sec translocon consists of the integral membrane proteins SecY, SecE, and SecG (38). SecY and SecE, but not SecG, are essential for viability (38). The crystal structure of the SecYEβ complex from the archaeon *Methanococcus jannaschii* suggests that the 10 transmembrane segments of *E. coli* SecY can be divided into two halves (transmembrane segments 1 to 5 and 6 to 10) that are clamped together by the third and essential transmembrane segment of SecE (65). Recent evidence suggests that although a SecYEG heterotrimer serves as the protein translocation channel, multiple SecYEG heterotrimers may cooperate in protein translocation/insertion (40, 41, 48). SecA, an ATPase that is associated with the Sec translocon, drives the stepwise translocation of secretory proteins and large periplasmic loops of inner membrane proteins across the inner membrane (38). The Sec translocon-associated proteins SecD, SecF, and YajC form a complex that facilitates protein translocation, but they are not required for viability (38). The SecDF-YajC complex is thought to mediate the interplay between the SecYEG protein-conducting channel and YidC, an essential inner membrane protein which appears to be involved in the transfer of transmembrane segments from the Sec translocon into the lipid bilayer (34, 37, 46, 71). Evidence is accumulating that YidC by itself can also mediate the insertion of a subset of membrane proteins (34, 37).

The notion that most secretory and inner membrane proteins require the Sec translocon for translocation and/or insertion is based on studies using focused approaches and a limited number of model proteins, such as the outer membrane protein OmpA and the inner membrane protein FtsQ (21, 48). To study Sec translocon-mediated protein translocation and insertion in a more global way, we performed a comparative subproteome analysis of cells depleted of SecE and cells expressing normal levels of SecE. This approach allowed us to investigate protein mislocalization, aggregation, and changes in the composition of the outer and inner membrane proteomes of cells with strongly reduced Sec translocon levels (1). Our analysis showed that upon SecE depletion, secretory proteins aggregate in the cytoplasm and the cytoplasmic σ^{32} stress response is induced. This response is activated upon protein

* Corresponding author. Mailing address: Center for Biomembrane Research, Department of Biochemistry and Biophysics, Stockholm University, SE-106 91 Stockholm, Sweden. Phone: 46-8-162420. Fax: 46-8-153679. E-mail: degier@dbb.su.se.

† Supplemental material for this article may be found at http://jb.asm.org/.

‡ Present address: Department of Chemistry and Biochemistry, University of California Los Angeles, Box 951569, Los Angeles, CA 90095-1569.

▽ Published ahead of print on 22 February 2008.

misfolding/aggregation in the cytoplasm (4). Interestingly, the effects of reduced Sec translocon levels on the proteomes of the outer and inner membranes were different. Both the steady-state levels and the translocation efficiencies of most outer membrane proteins were reduced. The inner membrane proteome appeared to be differentially affected by the depletion of SecE. The levels of some proteins were reduced in the inner membrane, while the levels of other proteins were unaffected or increased. Notably, our analysis indicated that all integral inner membrane proteins whose levels were unaffected or increased upon SecE depletion lack large periplasmic domains and/or contain only one or two transmembrane segments. This study provides several testable hypotheses and new substrates that can be used to further discover guiding principles for protein translocation and insertion.

MATERIALS AND METHODS

Strains and culture conditions. In *E. coli* strain CM124, the chromosomal copy of the gene encoding SecE is inactivated and placed on a plasmid under control of the promoter of the *araBAD* operon (60). CM124 was cultured in standard M9 minimal medium supplemented with thiamine (10 mM), all amino acids (0.7 mg/ml) except methionine and cysteine, glucose (0.2%, wt/vol), arabinose (0.2%, wt/vol), and ampicillin (100 μg/ml) at 37°C in an Innova 4330 (New Brunswick Scientific) shaker at 180 rpm. Overnight cultures were washed in fresh medium without arabinose and then diluted to an optical density at 600 nm (OD_{600}) of 0.035 in fresh medium without arabinose to deplete the SecE in the cells ("SecE-depleted cells") or in medium containing 0.2% arabinose to induce expression of SecE ("control cells"). Cells were cultured for 6 h. Growth was monitored by measuring the OD_{600} with a Shimadzu UV-1601 spectrophotometer.

SDS-PAGE, 1D BN-PAGE, and immunoblot analysis. Immunoblot analysis was used to monitor the levels of the SecE, SecY, SecG, SecA, SecD, SecF, YidC, FtsQ, Lep, F_ob, F_oc, DegP, Skp, OmpA, OmpF, PhoE, IbpA/B, SecB, Ffh, and PspA proteins in whole-cell lysates and/or inner membranes. Whole cells (0.1 OD_{600} unit) and purified inner membranes (5 μg of protein) were solubilized in Laemmli solubilization buffer and separated by sodium dodecyl sulfate (SDS)-polyacrylamide gel electrophoresis (PAGE). Proteins were transferred from the polyacrylamide gels to a polyvinylidene difluoride (PVDF) membrane (Millipore). Membranes were blocked and decorated with antisera to the components listed above essentially as described previously (26). Proteins were detected with horseradish peroxidase-conjugated secondary antibodies (Bio-Rad) using the ECL system according to the instructions of the manufacturer (GE Healthcare) and a Fuji LAS 1000-Plus charge-coupled device camera. Blots were quantified using the Image Gauge 3.4 software (Fuji). Experiments were repeated with three independent samples. Changes were calculated as follows. The average band intensity for samples of SecE-depleted cells was divided by the average band intensity for samples of control cells. For secretory proteins (DegP, PhoE, Skp, OmpA, and OmpF), the percentage of the precursor and mature forms detected in samples of SecE-depleted cells relative to the mature form detected in samples of control cells was determined. It should be noted that for secretory proteins only the mature form was detected in control cells.

To monitor the abundance of the SecYEG protein-conducting channel, inner membrane vesicles were subjected to one-dimensional (1D) blue native PAGE (BN-PAGE) (58), followed by immunoblot analysis using antibodies to SecY, SecE, and SecG. Inner membrane pellets (20 μg of protein) were solubilized in buffer containing 750 mM 6-aminocaproic acid, 50 mM bis-Tris-HCl (pH 7.0 at 4°C), and freshly prepared 0.5% (wt/vol) *n*-dodecyl-β-D-maltopyranoside (DDM). After removal of unsolubilized material by centrifugation (100,000 × *g*, 30 min), Serva Blue G was added to a final concentration of 0.5% (wt/vol), and the samples were loaded onto the first-dimension gel. The 0.02% Serva Blue G cathode buffer used for BN-PAGE was changed to 0.002% Serva Blue G cathode buffer after one-third of the run in order to prevent excessive binding of Coomassie brilliant blue dye to the PVDF membrane in the subsequent transfer step. Ferritin (440 and 880 kDa), aldolase (158 kDa), and albumin (66 kDa) (GE Healthcare) were used as molecular mass markers. Proteins were transferred to a PVDF membrane, detected by antisera to SecY, SecE, and SecG, and quantified as described above.

Protein translocation assay. Translocation of OmpA was monitored essentially as described previously (25). Cultures corresponding to 0.4 OD_{600} unit were labeled with [^{35}S]methionine (60 μCi/ml [1 Ci = 37 GBq]) for 30 s, and this was followed by precipitation in 10% trichloroacetic acid either immediately or after a chase with cold methionine (final concentration, 0.5 mg/ml) for 3 and 10 min. Trichloroacetic acid-precipitated samples were washed with acetone, resuspended in 10 mM Tris-HCl (pH 7.5), 2% SDS, and immunoprecipitated with antiserum to OmpA. The OmpA precipitate was subjected to standard SDS-PAGE analysis. Gels were scanned with a Fuji FLA-3000 phosphorimager and quantified as described above. The percentage of the precursor and the mature form of OmpA detected in the SecE-depleted cells relative to the mature OmpA detected in the control cells was determined.

Flow cytometry and microscopy. Analysis of SecE-depleted and control cells using flow cytometry was carried out using a FACSCalibur instrument (BD Biosciences). To assess viability, cells were incubated in the dark at room temperature with 30 μM propidium iodide for 15 min (31). For staining of the inner membrane, cells were cultured at 37°C for 30 min with the membrane-specific fluorophore FM4-64 (Invitrogen) at a concentration of 2 μM (24). Cultures were diluted in ice-cold phosphate-buffered saline to a final concentration of approximately 10^6 cells per ml. A low flow rate was used throughout data collection with an average of 250 events per s. Forward and side scatter acquisition was used for comparison of cell morphology (5). Data acquisition was performed using CellQuest software (BD Biosciences), and data were analyzed with FloJo software (Tree Star).

For microscopy, cells were mounted on a slide and immobilized in 1% low-melting-temperature agarose. Microscopy was performed with a Zeiss Axioplan2 fluorescence microscope equipped with an Orca-ER camera (Hamamatsu). Images were processed with the AxioVision 4.5 software from Zeiss.

Isolation and analysis of protein aggregates. Protein aggregates were extracted from whole cells essentially as described previously (59). Cells corresponding to 75 OD_{600} units were used for each aggregate extraction. The protein contents of cell lysates and aggregate extracts were determined using the bicinchoninic acid assay according to the instructions of the manufacturer (Pierce). Aggregates isolated from 0.75 OD_{600} unit were analyzed by SDS-PAGE using 24-cm-long 8 to 16% acrylamide gradient gels. Gels were stained with Coomassie brilliant blue R-250, and proteins were identified by mass spectrometry (MS) as described below. The aggregate fraction was also subjected to in-solution digestion, followed by nano-liquid chromatography-electrospray ionization-tandem MS (nano-LC-ESI-MS/MS) as described below.

Isolation of inner and outer membranes. Inner and outer membranes were isolated essentially as described previously (67). Membrane fractions used for immunoblot analysis were prepared from nonradiolabeled cultures. Membrane fractions used for analysis by two-dimensional gel electrophoresis (2DE) (outer membranes) or two-dimensional (2D) BN/SDS-PAGE (inner membranes) were prepared from a mixture of labeled and unlabeled cells as outlined in Fig. S1 in the supplemental material. Cells corresponding to 1,000 OD_{600} units were cultured as described above. An aliquot (10 OD_{600} units) of cells was labeled with [^{35}S]methionine (60 μCi/ml [1 Ci = 37 GBq]) for 1 min, and this was followed by a chase for 10 min with cold methionine (final concentration, 5 mg/ml). Labeled cells were subsequently collected by centrifugation, and cell pellets were snap frozen in liquid nitrogen. The remainder of the cells (990 OD_{600} units) was harvested by centrifugation and washed once with buffer K (50 mM triethanolamine [TEA], 250 mM sucrose, 1 mM EDTA, 1 mM dithiothreitol [DTT]; pH 7.5). The cell pellets were snap frozen in liquid nitrogen and stored at −80°C. Before the cells were broken, labeled and unlabeled cells from the same culture were pooled in a 1:100 ratio. The resulting mixture was resuspended in 8 ml buffer K supplemented with 0.1 mg/ml Pefabloc and 5 μg/ml DNase and lysed by using a French press (two cycles; 18,000 lb/in^2). The unbroken cells were removed from the lysate by centrifugation at 8,000 × *g* for 20 min, and the total membrane fraction was collected by centrifugation at 100,000 × *g* for 1 h. The membrane pellet was resuspended in 1 ml of buffer M (50 mM TEA, 1 mM EDTA, 1 mM DTT; pH 7.5) and loaded on top of a six-step sucrose gradient consisting of (from bottom to top, in buffer M) 0.5 ml of 55% (wt/wt) sucrose, 1.5 ml of 50% (wt/wt) sucrose, 1.5 ml of 45% (wt/wt) sucrose, 2.5 ml of 40% (wt/wt) sucrose, 2.5 ml of 35% (wt/wt) sucrose, and 2.5 ml of 30% (wt/wt) sucrose. After centrifugation at 210,000 × *g* for 15 h, the inner membrane and outer membrane fractions were collected from the 35 and 45% sucrose layers, respectively. The collected fractions were diluted in TEA buffer (50 mM TEA, 1 mM DTT; pH 7.5) to obtain a sucrose concentration less than 10%. Membranes were collected by centrifugation at 170,000 × *g* for 1 h and subsequently resuspended in buffer L (50 mM TEA, 250 mM sucrose, 1 mM DTT; pH 7.5). The inner membrane fraction was snap frozen in liquid nitrogen, and the outer membrane fraction was washed in 0.1 M sodium carbonate as described previously (5). Protein concentrations were determined using the bicinchoninic acid assay. Samples were stored at −80°C.

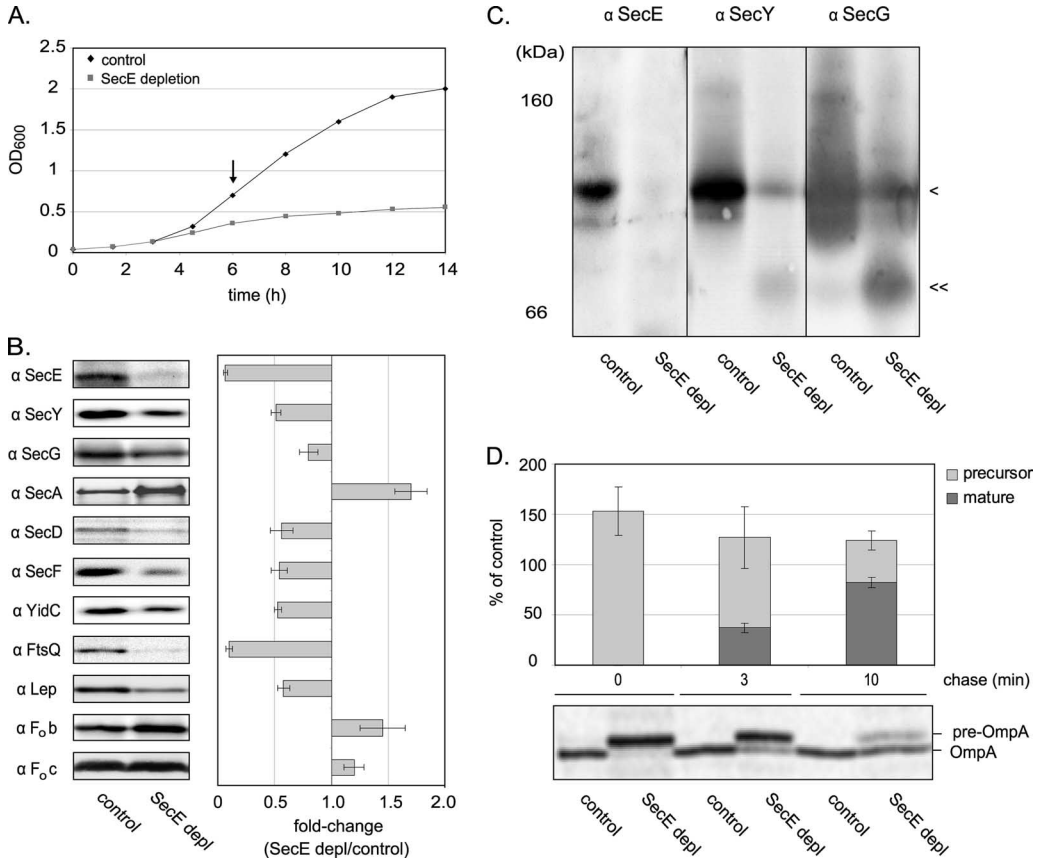

FIG. 1. Effect of SecE depletion on growth, steady-state levels of Sec components, model inner membrane proteins, and OmpA translocation. (A) Effect of SecE depletion on cell growth. Growth of CM124 cultured in the presence (control) and absence (SecE depletion) of 0.2% arabinose was monitored by measuring the OD_{600}. (B) Quantification of the steady-state levels of SecE, SecY, SecG, SecA, SecD, SecF, and YidC, as well as the model substrates FtsQ, Lep, F_ob, and F_oc, in the inner membrane of SecE-depleted (SecE depl) and control cells. Inner membranes from SecE-depleted and control cells were subjected to SDS-PAGE followed by immunoblot analysis with antibodies to the components listed above. The graph indicates the average changes in the intensities of the bands upon SecE depletion compared to the control. The quantification was based on three independent samples. α, antibody. (C) Analysis of the integrity and abundance of the SecYEG complex. Inner membranes from SecE-depleted and control cells were subjected to BN-PAGE analysis followed by detection of SecE, SecY, and SecG by immunoblotting. The position of the SecYEG trimer is indicated by one arrowhead, and the position of the putative SecYG complex is indicated by two arrowheads. (D) Effect of depletion of SecE on the translocation of the major outer membrane protein OmpA. SecE-depleted and control cells were labeled with [^{35}S]methionine for 30 s and, after cold methionine was added, chased for 3 and 10 min. OmpA was immunoprecipitated and subjected to standard SDS-PAGE analysis, and labeled material was detected by phosphorimaging. The bars in the graph indicate the percentages of the precursor and mature forms of OmpA detected in the SecE-depleted cells compared to the amounts of mature OmpA detected in the control cells. The experiment was repeated three times.

2DE. Whole-cell lysates (1 OD_{600} unit) and [^{35}S]methionine-labeled outer membranes (185 μg of protein) isolated by density centrifugation were analyzed by 2DE using isoelectric focusing in the first dimension and SDS-PAGE in the second dimension (5). Gels used for comparative analysis of whole-cell lysates were stained with high-sensitivity silver stain (47). Gels used for comparative analysis of the outer membrane proteome and all gels used for MS-based identification of proteins were stained with colloidal Coomassie brilliant blue (45). Most proteins in the outer membrane gels gave rise to multiple spots with the same molecular mass but different pIs. This phenomenon was also observed in the outer membrane map of *E. coli* constructed by Molloy et al. (43). Most "trains of spots" are caused by modifications induced during sample preparation (7), likely due to stepwise deamidation of the asparagine and glutamine residues, resulting in loss of 1 Da and a net loss of one positive charge (73).

Analysis of cytoplasmic membrane fractions by 2D BN/SDS-PAGE. Comparative 2D BN/SDS-PAGE was performed as described previously (67). In short, [^{35}S]methionine-labeled inner membranes (100 μg of protein) were solubilized in 0.5% (wt/vol) DDM and subjected to BN electrophoresis in the first dimension and denaturing SDS-PAGE in the second dimension. For calibration, ferritin (440 and 880 kDa), aldolase (158 kDa), and albumin (66 kDa) (GE Healthcare) were used as molecular mass markers. Gels were stained with Coomassie brilliant blue R-250 (5).

Image analysis and statistics. Stained gels were scanned using a GS-800 densitometer from Bio-Rad. Radiolabeled gels were scanned with a Fuji FLA-3000 phosphorimager. Spots were detected, matched, and quantified using PDQuest software, version 8.0 (Bio-Rad). The analysis of Coomassie brilliant blue-stained and [^{35}S]methionine-labeled outer and inner membrane proteins was done using the same set of gels. In all cases, each analysis set consisted of at least three gels for each replicate group (i.e., SecE-depleted cells and the control). Each gel in a set represented an independent sample (i.e., a sample from a different bacterial colony, culture, and membrane preparation). Independent samples were subjected to 2DE or 2D BN/SDS-PAGE and image analysis in parallel (i.e., en groupe). Spot quantities were normalized using the "total intensity of valid spots" method to compensate for non-expression-related variations in spot quantities between gels (there were no significant variations in the total spot quantity between the two groups [SecE depletion and control]). Since protein aggregates can cosediment with outer membranes during density gradient centrifugation, an additional normalization step was required for analysis of the outer membrane gels (35, 39). First, to distinguish between outer membrane

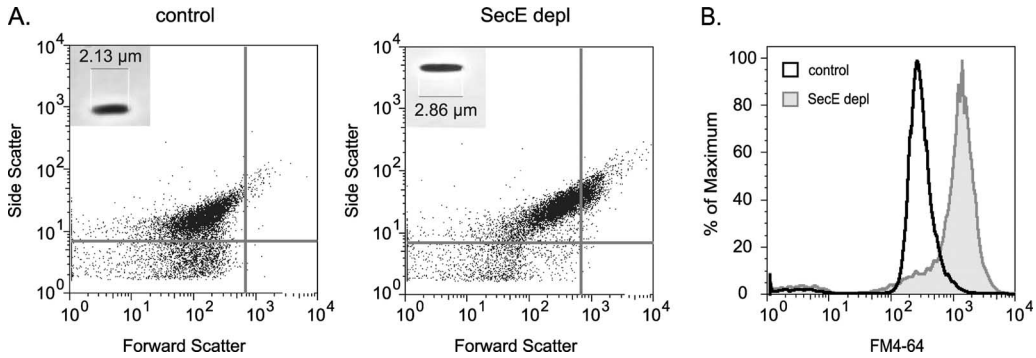

FIG. 2. Flow cytometric properties of control and SecE-depleted (SecE depl) cells. SecE-depleted and control cells were analyzed by flow cytometry. (A) Size of the population (forward scatter) plotted versus granularity (side scatter) for SecE-depleted and control cells. The insets show microscope images of representative cells from the SecE-depleted and control cultures. Cell length is indicated by scale bars. (B) Histograms representing the fluorescence of cultures stained with the membrane-specific fluorophore FM4-64.

spots and contaminating aggregate spots, the outer membrane fractions from SecE-depleted and control cells were subjected to aggregate extraction as described above. The resulting extracts were analyzed by 2DE, and proteins in the aggregates were visualized by staining with colloidal Coomassie brilliant blue. Spots detected in the gels of the aggregate extract were removed from the outer membrane analysis set if the intensity of a spot in the aggregate gel was more than 5% of the intensity of the spot detected in the outer membrane gels. The quantities of the remaining spots were normalized using the "total quantity of valid spots" method to correct for the contribution of protein aggregates on protein loading. Spots detected by means of phosphorimaging were normalized using the correction value calculated for the corresponding Coomassie brilliant blue-stained gel to allow correction for errors in protein loading while differences in labeling efficiency between the control and SecE-depleted cells were retained. The changes for spots matched in different gels were calculated by dividing the average spot intensity for gels with SecE-depleted samples by the corresponding value for gels with control samples. PDQuest was set to detect differences that were found to be statistically significant using the Student *t* test and a 95% level of confidence, including qualitative differences "on-off responses") present in all gels in a group. Saturated spots were excluded from the analysis. In order to present qualitative responses in bar diagrams with a logarithmic scale, on and off responses were given values of 100- and 0.01-fold, respectively (67).

MS-based identification of proteins. Coomassie brilliant blue-stained protein spots or bands were excised, washed, and digested with modified trypsin, and peptides were extracted manually or automatically (ProPic and Progest; Genomic Solutions, Ann Arbor, MI). Peptides were applied to a matrix-assisted laser desorption ionization (MALDI) target plate as described previously (50). Mass spectra were obtained automatically by MALDI-time of flight (TOF) MS in reflectron mode (Voyager-DE-STR; PerSeptive Biosystems, Framingham, MA), followed by automatic internal calibration using tryptic peptides from autodigestion. The spectra were analyzed for monoisotopic peptide peaks (*m*/*z* range, 850 to 5,000) using the software MoverZ from Genomic Solutions (http://65.219.84.5/moverz.html) with a signal-to-noise ratio threshold of 3.0. Matrix and/or autoproteolytic trypsin fragments were not removed. Spectral annotations (in particular, assignments of monoisotopic masses) were verified by manual inspection for a large number of measurements. The resulting peptide mass lists were used to search the Swiss-Prot 45.0 database (release 10/04) for *E. coli* with Mascot (v2.0) in automated mode (www.matrixscience.com), using the following search parameters or criteria: significant protein MOWSE score at $P < 0.05$; no missed cleavages allowed; variable methionine oxidation; fixed carbamidomethylation of cysteines; and a minimum mass accuracy of 50 ppm. The search result pages were extracted and analyzed by using an additional in-house filter (Q. Sun and K. J. van Wijk, unpublished) by applying the following three criteria for positive identification: (i) minimum MOWSE score of ≥50; (ii) ≥4 matching peptides with an error distribution within ±25 ppm; and (iii) ≥15% sequence coverage. The false-positive rates were less than 1%, as determined by searching with the .pkl list against the *E. coli* database (Swiss-Prot) mixed with a randomized version of the *E. coli* database, generated using a Perl script from Matrix Science.

Aggregate fractions isolated from whole cells were subjected to in-solution digestion with modified trypsin (51). The resulting peptide mixtures were analyzed by nano-LC-ESI-MS/MS in automated mode using a quadruple/orthogonal-acceleration TOF tandem mass spectrometer (Q-TOF; Micromass). The spectra were used to search the Swiss-Prot database (downloaded locally) automated using Mascot (v2.0) (www.matrixscience.com). When Mascot was searched, the maximum precursor and fragment errors were 1.2 and 0.6 Da, respectively. For all significant MS/MS identifications based on a single peptide, spectral quality and matching y and b ion series were manually verified (see Fig. S3 in the supplemental material).

RESULTS

Characterization of the SecE depletion strain CM124. *E. coli* strain CM124 was used to study the consequences of depletion of SecE for protein insertion and translocation. In CM124, the chromosomal copy of *secE* is inactivated, and a copy of *secE* is placed on a plasmid under control of the promoter of the *araBAD* operon (60). Cells were cultured aerobically in M9 minimal medium in the presence of arabinose to induce expression of SecE (these cells are referred to in this paper as "control cells") and in the absence of arabinose to deplete cells of SecE. Growth was monitored by measuring the OD_{600} (Fig. 1A). As expected, the growth of CM124 cells cultured in the absence of arabinose was much slower than the growth in control cultures.

For all experiments, cells were harvested 6 h after inoculation. At this time point, control cells were in the mid-log phase with an OD_{600} of 0.8, and SecE-depleted cells reached an OD_{600} of 0.3 to 0.4. Inner membranes were isolated from control cells and SecE-depleted cells, and the levels of SecE, SecY, SecG, SecA, SecD, SecF, and YidC were analyzed by immunoblotting. The level of SecE in the membrane of depleted cells was less than 10% of the level of the SecE detected in membranes prepared from control cells. The levels of SecY and SecG in SecE-depleted membranes were reduced to 50 and 20%, respectively (Fig. 1B). SecY is degraded by the FtsH protease in the absence of SecE (1). Since the Sec translocon is composed of SecY, SecE, and SecG in a 1:1:1 ratio (65), this indicates that the SecE-depleted membrane contains pools of SecY and SecG, which are not in a SecYEG complex. The abundance of SecYEG heterotrimers in SecE-depleted membranes was monitored by BN-PAGE combined with immunoblotting (Fig. 1C). For this purpose, inner membranes prepared from SecE-depleted and control cells were solubilized in 0.5% DDM (8). Upon depletion of SecE, only a minute

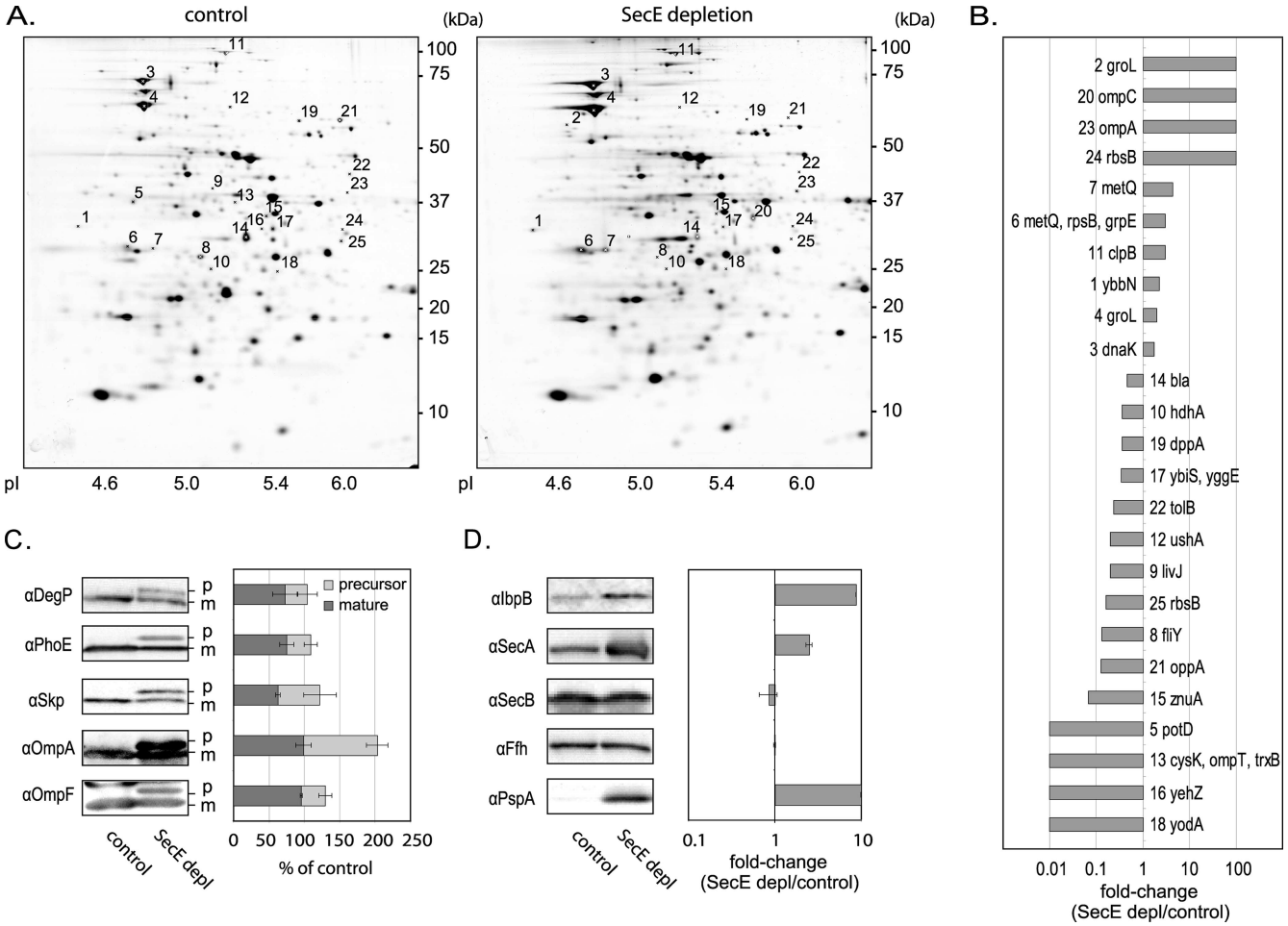

FIG. 3. Analysis of whole-cell lysates of SecE-depleted and control cells by 2DE and immunoblotting. (A) Comparative 2DE analysis of total lysates from SecE-depleted and control cells. Proteins from 1 OD_{600} unit of solubilized cells were separated by 2DE. Proteins were visualized by silver staining, and differences between SecE-depleted and control cells were analyzed using PDQuest. Twenty-five spots were significantly ($P < 0.05$) affected by SecE depletion. Proteins were identified by MALDI-TOF MS and PMF using spots excised from gels stained with Coomassie brilliant blue (Table 1; see Table S1 in the supplemental material). If several proteins were identified in the same spot, the first gene listed corresponds to the gene with the highest Mascot MOWSE score. Primary gene designations were obtained from Swiss-Prot (www.expasy.org). Annotated spots were matched on the silver-stained gels shown using PDQuest. (B) Graph showing the changes in spots that are significantly ($P < 0.05$) affected by SecE depletion. Changes were calculated by determining the average spot intensities in SecE-depleted samples (SecE depl)/average spot intensities in control samples. A change of 100-fold indicates that a spot was detected only in SecE-depleted samples ("on response"), and a change of 0.01-fold indicates that a spot was detected only in the control samples ("off response"). (C) Quantification of the precursor (p) and mature (m) forms of secretory proteins in SecE-depleted and control cells by immunoblotting. Whole cells were subjected to SDS-PAGE followed by immunoblot analysis with antibodies to two periplasmic proteins (DegP and Skp) and three outer membrane proteins (OmpA, OmpF, and PhoE). The bars in the graph indicate the percentages of the precursor and mature forms of the proteins detected in the SecE-depleted cells compared to the mature form detected in the control cells. The quantification was based on three independent samples. α, antibody. (D) Quantification of the levels of IbpA/B, SecA, Ffh, SecB, and PspA in whole cells. SecE-depleted and control cells were subjected to SDS-PAGE followed by immunoblot analysis with antibodies to the components listed above. The graph shows the changes calculated by determining the average band intensities detected in SecE-depleted cells/average band intensities detected in control cells. The quantification was based on three independent samples.

amount of the SecYEG heterotrimer could be detected. Interestingly, a complex that most likely represented a SecYG heterodimer could be detected in membranes of SecE-depleted cells but not in control membranes.

The amount of SecA was almost doubled in SecE-depleted membranes (Fig. 1B) (44), whereas the levels of SecD, SecF, and YidC were reduced by approximately 50%. In addition, the steady-state levels of the well-studied model proteins FtsQ, Lep, F_ob, and F_oc were monitored by immunoblotting (Fig. 1B) (16, 21, 63, 66, 72). As expected, the accumulation levels of the Sec translocon-dependent inner membrane proteins FtsQ and Lep were strongly reduced upon SecE depletion, whereas the level of the Sec translocon-independent protein F_oc was slightly increased. To our surprise, the level of F_ob was somewhat increased, contradicting a previous proposition that translocation of F_ob is dependent on the Sec translocon (72).

Pulse-chase experiments showed that translocation of OmpA was delayed but not abolished upon SecE depletion (Fig. 1D). Possibly as a response to compensate for the delayed

TABLE 1. Comparative 2D gel analysis and MS identification of proteins from total lysates of SecE-depleted and control cells[a]

Spot[b]	Gene[c]	Protein						
		Designation or function[d]	Localization[e]	Predicted mol wt (10^3) (precursor/mature)[f]	Predicted pI (precursor/mature)[g]	Observed mol wt (10^3)[h]	Observed pI[i]	Change (fold) (SecE depleted/control)[j]
1	*ybbN*	YbbN	c	31.8	4.5	31.8	4.5	2.23
2	*groL*	60-kDa chaperonin GroEL[k]	c	57.3	4.85	55.3	4.68	100
3	*dnaK*	Chaperone protein DnaK	c	69.1	4.83	68.9	4.83	1.74
4	*groL*	60-kDa chaperonin GroEL[k]	c	57.3	4.85	60.2	4.83	1.96
5	*potD*	Spermidine/putrescine-binding periplasmic protein	p	38.9/36.5	5.24/4.86	35.87	4.76	0.01
6	*metQ*	D-Methionine-binding lipoprotein MetQ	im lp/om lp	38.9/36.5	5.24/4.86	27.25	4.73	2.96
6	*rpsB*	30S ribosomal protein S2	c	26.7	6.61	27.25	4.73	2.96
6	*grpE*	Protein GrpE	c	21.8	4.68	27.25	4.73	2.96
7	*metQ*	D-Methionine-binding lipoprotein MetQ	im lp/om lp	38.9/36.5	5.24/4.86	27.4	4.88	4.32
8	*fliY*	Cystine-binding periplasmic protein	p	29.3/26.1	6.22/5.29	25.58	5.18	0.13
9	*livJ*	Leu/Ile/Val-binding protein	p	39.1/36.8	5.54/5.28	38.7	5.22	0.20
10	*hdhA*	7-Alpha-hydroxysteroid dehydrogenase	c	26.8	5.22	23.39	5.21	0.37
11	*clpB*	Chaperone ClpB	c	95.6	5.37	79.12	5.29	2.96
12	*ushA*	Protein UshA	p	60.8/58.2	5.47/5.4	59.65	5.31	0.20
13	*cysK*	Cysteine synthase A	amb	34.5	5.83	35.47	5.34	0.01
13	*ompT*	Protease 7	om	35.6/33.5	5.76/5.38	35.47	5.34	0.01
13	*trxB*	Thioredoxin reductase	c	34.6	5.3	35.47	5.34	0.01
14	*bla*	Beta-lactamase TEM	p	31.5/28.9	5.69/5.46	29.8	5.39	0.46
15	*znuA*	High-affinity zinc uptake system protein ZnuA	p	33.8/31.1	5.61/5.44	33.29	5.52	0.07
16	*yehZ*	Hypothetical protein YehZ	p	32.6/30.2	5.82/5.56	31.19	5.48	0.01
17	*ybiS*	YbiS	p	33.42/30.86	5.99/5.6	31.19	5.57	0.34
17	*yggE*	Hypothetical protein YggE	p	26.6/24.5	6.1/5.60	31.19	5.57	0.34
18	*yodA*	Metal-binding protein YodA	p	24.8/22.3	5.91/5.66	23.15	5.6	0.01
19	*dppA*	Periplasmic dipeptide transport protein	p	60.3/57.4	6.21/5.75	55.21	5.74	0.36
20	*ompC*	Outer membrane protein C	om	40.4/38.3	4.58/4.48	32.71	5.76	100
21	*oppA*	Periplasmic oligopeptide-binding protein	p	60.97/58.5	6.05/5.85	54.94	6.02	0.13
22	*tolB*	TolB	p	46.0/43.6	6.98/6.14	41.31	6.09	0.23
23	*ompA*	Outer membrane protein A	om	37.2/35.2	5.99/5.60	37.3	6.07	100
24	*rbsB*	D-Ribose-binding periplasmic protein	p	31.0/28.5	6.85/5.99	30.67	6.03	100
25	*rbsB*	D-Ribose-binding periplasmic protein	p	31.0/28.5	6.85/5.99	28.46	6.02	0.17

[a] Spots visualized by silver staining (Fig. 3A) were quantified and compared using PDQuest. Spot quantities were normalized using the "total quantity of valid spot" method. Changes of 0.01- and 100-fold correspond to spots that are missing ("off response") or turned on ("on response") in the SecE-depleted cells, respectively. All spots that were significantly ($P < 0.05$) changed upon SecE depletion were excised from gels stained with colloidal Coomassie brilliant blue, and proteins were identified by MALDI-TOF MS and PMF.

[b] The numbers correspond to the spots in the 2D gel images in Fig. 3A.

[c] Gene designations in the Swiss-Prot database for *E. coli*.

[d] Protein designations in the Swiss-Prot database for *E. coli*.

[e] Localization based on the information given in the Swiss-Prot database for *E. coli*. Unknown localizations were predicted by PSORT. Abbreviations: amb, ambiguous; c, cytoplasmic; im lp, inner membrane lipoprotein; om, outer membrane; om lp, outer membrane lipoprotein; p, periplasmic.

[f] Protein sizes predicted from amino acid sequences. Two sizes are given for secretory proteins; the first size is the size of the precursor form, and the second size is the size of the mature form of the protein.

[g] pIs predicted from the amino acid sequence. Two values are given for secretory proteins; the first value is the pI for the precursor form, and the second value is the pI for the mature form of the protein.

[h] Sizes of proteins calculated from the spot positions on the 2D gels used for the analysis.

[i] pIs of proteins calculated from the spot positions on the 2D gels used for the analysis.

[j] Changes expressed as the ratio of the average intensity of significantly ($P < 0.05$) affected spots in the SecE depletion gels to the average intensity of matched spots in the control gels.

[k] The occurrence of different forms of GroEL is explained in reference 55.

translocation, the total (pre-)OmpA accumulation was initially higher in the SecE-depleted cells than in the control cells.

Flow cytometry and microscopy. The integrity of the inner membrane of SecE-depleted and control cells was monitored using propidium iodide staining combined with flow cytometry (31). This analysis showed that 9.0% ± 2.0% of SecE-depleted cells stained fluorescently red with propidium iodide, compared to 1.0% ± 0.3% of the control cells, indicating that SecE depletion had only a minor impact on the integrity of the inner membrane. Furthermore, we detected small increases in both the forward scatter and side scatter of cells depleted of SecE (Fig. 2A). This indicates that SecE-depleted cells are slightly bigger than control cells and most likely contain extra internal structures (i.e., extra membranes and/or protein aggregates). Light microscopy showed that SecE-depleted cells were slightly elongated compared to the control cells (Fig. 2A). Cellular membranes in SecE-depleted cells and control cells were stained with the fluorescent dye FM4-64 and analyzed by flow cytometry (24). SecE-depleted cells showed fourfold-greater fluorescence than control cells, indicating that there were increased amounts of membranes upon SecE depletion (Fig. 2B). This is in keeping with the observation that SecE depletion induces the formation of endoplasmic membranes (29).

SecE depletion leads to accumulation of secretory proteins in the cytoplasm and induction of the σ^{32} stress response. Whole-cell lysates of SecE-depleted and control cells were compared by using 2DE and immunoblot analysis. The comparative 2DE analysis was based on four biological replicates. Proteins were separated by using denaturing immobilized pH gradient (IPG) strips (pH 4 to 7) in the first dimension and by Tricine-SDS-PAGE in the second dimension. Gels were stained with silver or colloidal Coomassie brilliant blue, and spot volumes were compared using PDQuest. This analysis demonstrated that the volumes of 25 spots were significantly ($P < 0.05$) changed in the lysates of SecE-depleted cells compared to the control; the intensity increased for 10 spots and decreased for 15 spots. The affected spots were excised and used for protein identification by MALDI-TOF MS and peptide mass fingerprinting (PMF) (Fig. 3A and Table 1). Spot statistics and MS data are provided in Table S1 in the supplemental material. The effects of SecE depletion on protein accumulation levels are expressed as changes (SecE depletion/control) in Fig. 3B.

The accumulation levels of a number of secretory proteins (β-lactamase, DppA, FliY, LivJ, PotD, OmpT, OppA, TolB, UshA, YbiS, YehZ, YggE, YodA, and ZnuA) were reduced in SecE-depleted cells. Based on the pI and molecular weight, the spots corresponded to the processed forms of these proteins (Table 1). OmpC, MetQ, and OmpA were identified in spots that were stronger in lysates of SecE-depleted cells. The positions of the spots in which OmpC and MetQ were identified suggested that these spots contained degraded forms of these proteins. Based on pI and molecular weight, the OmpA spot likely contained pre-OmA. This conclusion was supported by an MS analysis (see Fig. S2 in the supplemental material). RbsB was identified in two spots, one high-intensity spot that was reduced upon SecE depletion and a faint spot that appeared only with SecE-depleted cells. It is likely that the high-intensity spot corresponded to the mature form of the protein and the faint spot corresponded to the precursor form. However, based on pI and molecular weight it was not possible to unambiguously determine this.

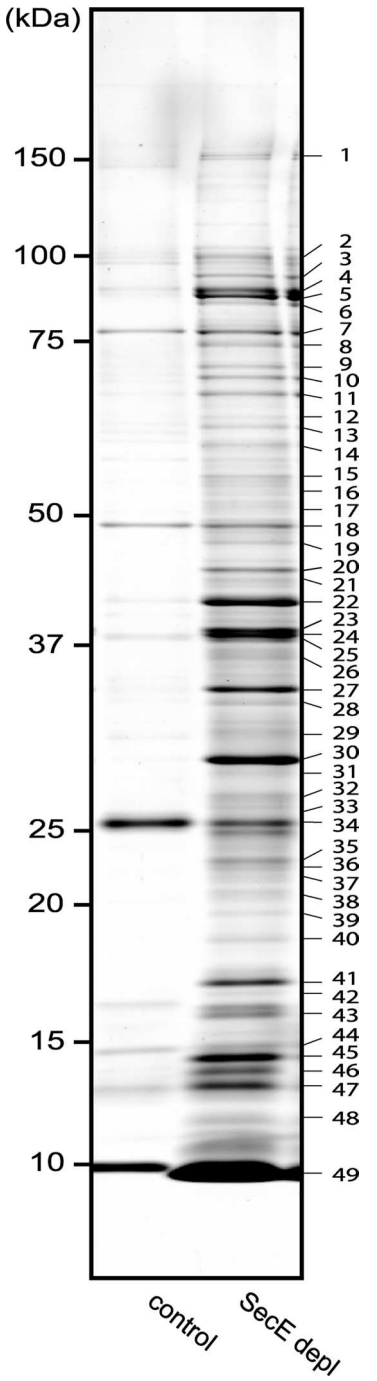

FIG. 4. Characterization of aggregates isolated from SecE-depleted cells (SecE depl). Aggregates isolated from SecE-depleted and control cells were analyzed by SDS-PAGE. Proteins were stained with colloidal Coomassie brilliant blue and subsequently identified by MALDI-TOF MS and PMF (Table 2; see Table S2 in the supplemental material). If several proteins were identified in the same band, the first gene listed corresponds to the protein with the highest Mascot MOWSE score.

To study the effect of SecE depletion in more detail, the accumulation levels of the periplasmic proteins DegP and Skp

TABLE 2. MS identification of proteins in aggregates isolated from lysates of SecE-depleted and control cells[a]

Band(s)[b]	Hit rank[c]	Gene[d]	Protein		
			Designation or function[e]	Localization or no. of transmembrane segments[f]	Predicted mol wt (10^3) (precursor/mature)[g]
2		*adhE*	Aldehyde-alcohol dehydrogenase	c	96.1
17		*atpA*	ATP synthase subunit alpha	c, im ass	55.4
22, 30, 33	1	*bla*	Beta-lactamase TEM	p	31.6/28.9
6		*clpB*	Chaperone ClpB	c	95.7
38	25	*crp*	Catabolite gene activator	c	23.6
28		*cysK*	Cysteine synthase A	amb	34.4
14		*cysN*	Sulfate adenylyltransferase subunit 1	c	52.6
25		*dacA*	Penicillin-binding protein 5	1*	40.3/38.3
23		*dacC*	Penicillin-binding protein 6	1*	43.6/40.8
	19	*degP*	Protease do	p	49.4/46.8
	23	*dnaJ*	Chaperone protein DnaJ	c	41.1
9		*dnaK*	Chaperone protein DnaK	c	69.1
42	13	*dps*	DNA protection during starvation protein	c	18.6
	14	*elaB*	ElaB	1	11.3
4, 5	6	*fusA*	Elongation factor G	c	77.6
18	12	*glgA*	Glycogen synthase	c	53.0
7, 36	17	*glgB*	1,4-Alpha-glucan branching enzyme	c	84.3
11		*glmS*	Glucosamine–fructose-6-phosphate aminotransferase	c	66.9
16		*guaB*	Inosine-5′-monophosphate dehydrogenase	c	52.0
11, 36		*htpG*	Chaperone protein HtpG	c	66.0
	21	*hupA*	DNA-binding protein HU-alpha	c	9.5
46, 47	16	*ibpA*	Small heat shock protein IbpA	c	15.8
23		*iscS*	Cysteine desulfurase	c	45.2
49	9	*lpp*	Major outer membrane lipoprotein	om lp	8.3/6.4
12		*lysS*	Lysyl-tRNA synthetase	c	57.6
4, 5	15	*metE*	5-Methyltetrahydropteroyltriglutamate-homocysteine methyltransferase	c	84.7
26		*mreB*	Rod shape-determining protein MreB	c	37.1
29		*nlpD*	Lipoprotein NlpD	im lp	40.2/37.5
27, 33, 34	3	*ompA*	Outer membrane protein A	om	37.2/35.2
24, 25	5	*ompC*	Outer membrane protein C	om	40.3/38.3
23, 24	18	*ompF*	Outer membrane protein F	om	39.3/37.1
24		*ompT*	Protease 7	om	35.5/33.5
41	8	*ompX*	Outer membrane protein X	om	18.7/16.2
13		*ptsI*	Phosphoenolpyruvate-protein phosphotransferase	c	63.6
35		*rplC*	50S ribosomal protein L3	c	22.2
37		*rplD*	50S ribosomal protein L4	c	22.1
40	24	*rplE*	50S ribosomal protein L5	c	20.5
39		*rplF*	50S ribosomal protein L6	c	18.9
44		*rplI*	50S ribosomal protein L9	c	15.8
1		*rpoC*	DNA-directed RNA polymerase β′ chain	c	155.1
10, 31		*rpsA*	30S ribosomal protein S1	c	61.2
32		*rpsB*	30S ribosomal protein S2	c	26.7
19, 21		*rpsC*	30S ribosomal protein S3	c	25.8
43		*rpsE*	30S ribosomal protein S5	c	17.5
40		*rpsG*	30S ribosomal protein S7	c	20.0
48	26	*rpsJ*	30S ribosomal protein S10	c	11.7
3		*secA*	Preprotein translocase subunit SecA	c	102.0
43, 44	10	*skp*	Chaperone protein Skp	p	17.7/15.7
45	4	*slyB*	Outer membrane lipoprotein SlyB	om lp	15.6/13.8
25		*spb*	Sulfate-binding protein	p	18.7/16.2
20	7	*tolB*	TolB	p	36.6/34.7
15		*tolC*	Outer membrane protein TolC	om	54.0/51.5
	2	*tufA*	Elongation factor Tu	c	43.3

Continued on following page

TABLE 2—*Continued*

Band(s)[b]	Hit rank[c]	Gene[d]	Protein		
			Designation or function[e]	Localization or no. of transmembrane segments[f]	Predicted mol wt (10^3) (precursor/mature)[g]
8		*typA*	GTP-binding protein TypA/BipA	c	67.4
	20	*yajG*	Uncharacterized lipoprotein YajG	om lp	21.0/19.0
35		*yfiO*	Lipoprotein YfiO	om lp	23.9/21.7
	11	*ygiW*	YgiW	p	14.0/12.0
	27	*yhjK*	YhjK	2	73.1
25	28	*yncE*	Hypothetical protein YncE	sec	38.6/35.3
	22	*yqjD*	Hypothetical protein YqjD	1	11.1
35		*yrbC*	YrbC	sec	23.9/21.7

[a] Protein aggregates were extracted from lysates of SecE-depleted and control cells. The protein content of the aggregates was analyzed by 1D electrophoresis followed by MALDI-TOF MS and PMF (Fig. 4; see Table S2 in the supplemental material) or nano-LC-ESI-MS/MS analysis of solubilized aggregates digested with trypsin (see Table S2 in the supplemental material).

[b] The numbers correspond to the bands in the 1D gel shown in Fig. 4.

[c] The ranking is based on the Mascot MOWSE score of proteins identified by in-solution digestion/nano-LC-ESI-MS/MS.

[d] Gene designations in the Swiss-Prot database for *E. coli*.

[e] Protein designations in the Swiss-Prot database for *E. coli*.

[f] Localization based on the information given in the Swiss-Prot database for *E. coli*. Unknown localizations were predicted by PSORT. For integral membrane proteins, the numbers of transmembrane segments are indicated. An asterisk indicates that the membrane-inserted segment may act as an anchor rather than as a true transmembrane segment. Abbreviations: amb, ambiguous; c, cytoplasmic; im ass, inner membrane associated; im lp, inner membrane lipoprotein; om, outer membrane; om lp, outer membrane lipoprotein; p, periplasmic; sec, secretory.

[g] Protein sizes were predicted from amino acid sequences. Two sizes are given for secretory proteins; the first size is the size of the precursor form, and the second size is the size of the mature form of the protein.

and the outer membrane proteins OmpA, OmpF, and PhoE were monitored by immunoblotting (Fig. 3C). Upon SecE depletion, the precursor forms of all these proteins were detected, indicating that there was accumulation in the cytoplasm due to hampered translocation. In the case of Skp, DegP, and PhoE, this was accompanied by significant decreases in the levels of the mature forms of the proteins. Interestingly, the total levels of DegP and Skp were not affected upon SecE depletion. This suggests that no extracytoplasmic stress responses are activated upon SecE depletion (57). The accumulation level of the mature form of OmpA was unaffected by the SecE depletion, while the accumulation level of OmpF was slightly reduced.

Upon SecE depletion, the accumulation levels of the σ^{32}-inducible, cytoplasmic chaperones DnaK, GroEL, and ClpB were increased (Fig. 3B). The up-regulation of DnaK and GroEL was confirmed by Western blotting (results not shown). Since the inclusion body proteins IbpA/B, SecA, SecB, and Ffh and phage shock protein A (PspA) were not identified in the 2D gels, we monitored their accumulation levels by immunoblotting (Fig. 3D). The level of the heat shock chaperones IbpA/B, also part of the σ^{32} regulon, was increased. Inclusion body proteins associate with protein aggregates and facilitate the extraction of proteins from aggregates by ClpB and DnaK (42). In agreement with the membrane blotting experiments (see above), the total level of SecA was increased in SecE-depleted cells, consistent with insufficient Sec translocon capacity (44). The accumulation levels of SecB and Ffh, two components involved in the targeting of secretory and inner membrane proteins, respectively, to the Sec translocon were both unaffected upon SecE depletion. This indicates that the protein targeting capacity is not affected upon SecE depletion. The level of PspA was monitored since the electrochemical potential plays an important role in protein translocation and the expression of PspA is up-regulated when it is affected. Similar to several other translocation and insertion mutant strains, a considerable PspA response was detected in SecE-depleted cells (18).

Taken together, the up-regulation of SecA and the accumulation of the unprocessed forms of secretory proteins indicate that protein translocation across the cytoplasmic membrane is strongly hampered. Furthermore, the accumulation levels of the σ^{32}-regulated chaperones DnaK, GroEL, ClpB, and IbpA/B are all increased upon SecE depletion, suggesting that reduced Sec translocon levels lead to protein misfolding/aggregation in the cytoplasm.

Accumulation of cytoplasmic protein aggregates in SecE-depleted cells. Protein aggregates were extracted from whole cells depleted of SecE. The aggregates from SecE-depleted cells contained 2.6% of the total cellular protein, compared to 0.3% in the control. The protein composition of the aggregates was analyzed by 1D gel electrophoresis followed by in-gel digestion and analysis by MALDI-TOF MS and PMF (Fig. 4; see Table S2 in the supplemental material) and by nano-LC-ESI-MS/MS of solubilized aggregates digested with trypsin (see Table S2 in the supplemental material). In total, 61 proteins were identified in aggregates isolated from cells depleted of SecE; these proteins included 19 secretory proteins, 5 inner membrane proteins, 36 cytoplasmic proteins, and 1 protein with a localization that could not be unambiguously predicted (Table 2). Among the identified cytoplasmic proteins were the chaperones IbpA, DnaK, and DnaJ. The MS/MS analysis revealed that at least four of the secretory proteins, OmpA, Lpp, β-lactamase, and SlyB, contained an uncleaved signal sequence (results not shown), indicating that these proteins aggregate in the cytoplasm rather than in the periplasm. The identified inner membrane proteins ElaB and YqjD contain one predicted transmembrane segment, while YhjK contains two such

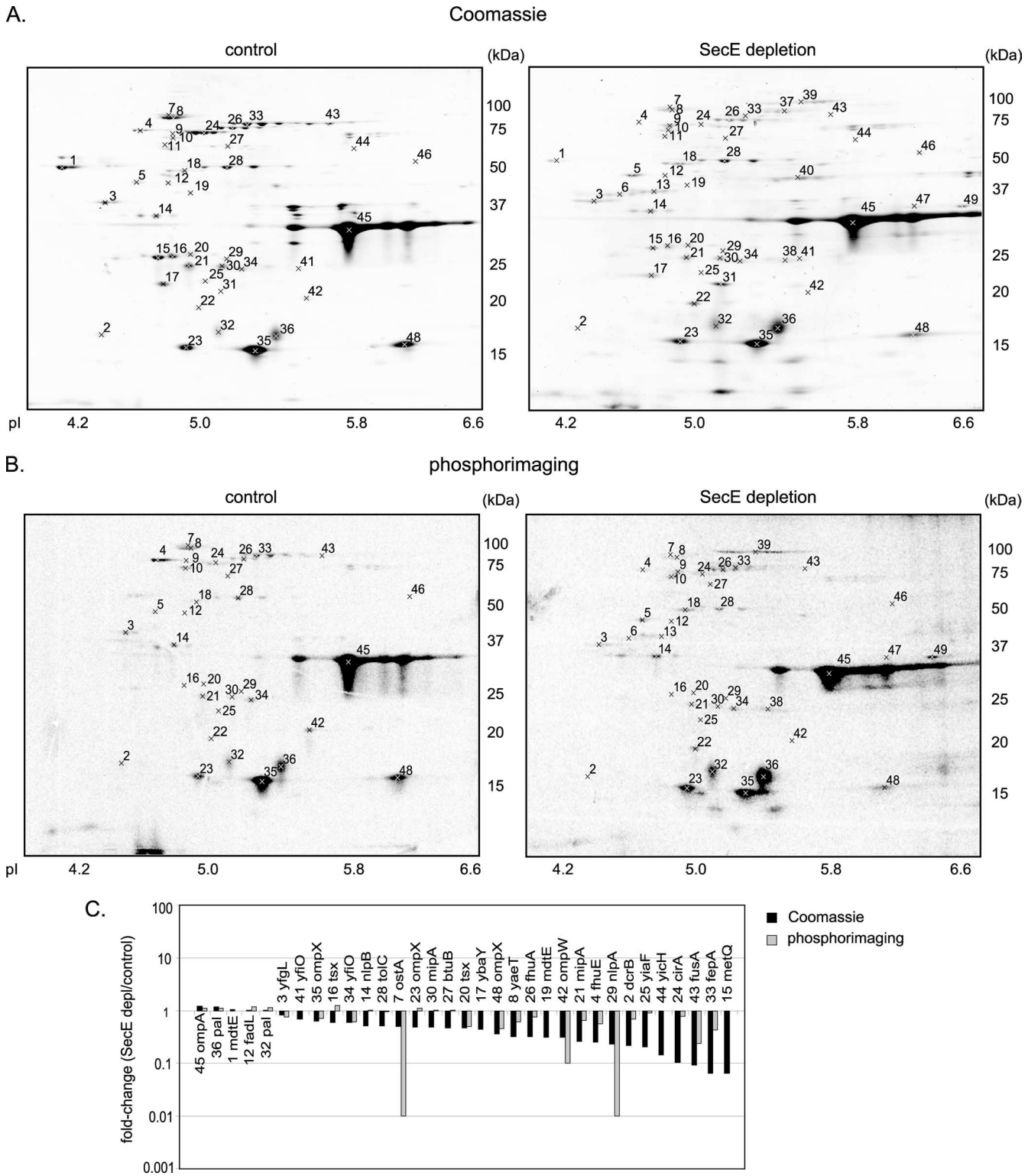

FIG. 5. 2DE analysis of the outer membrane proteome from SecE-depleted (SecE depl) and control cells. Cells were labeled with [^{35}S]methionine for 1 min, which was followed by a chase for 10 min with cold methionine. The outer membrane fractions were isolated by density centrifugation from a mixture of labeled and nonlabeled cells as outlined in Fig. S1 in the supplemental material (see Materials and Methods for details). The outer membrane fractions were used for separation by 2DE. Proteins were identified by MALDI-TOF MS and PMF using spots excised from with Coomassie brilliant blue-stained gels (Table 3; see Table S3 in the supplemental material). The outer membrane fraction of SecE-depleted cells was contaminated with aggregates that cosedimented with the outer membrane during density centrifugation (see Table S4 in the supplemental material). The spots corresponding to the proteins in these aggregates were identified and removed from the analysis set as described in Materials and Methods. Differences in the outer membrane proteomes of the SecE-depleted and control cells were analyzed using

segments. Penicillin-binding protein 5 (DacA) and penicillin-binding protein 6 (DacC) are probably attached to the inner membrane via a C-terminal amphiphilic α-helix (27). It is possible that the number of identified inner membrane proteins is somewhat underrepresented since the typical absence of lysine and arginine in the transmembrane domain regions leads to few peptides and large peptides upon digestion with trypsin (70).

The intensities of the bands in the gel shown in Fig. 4 were quantified to get an estimate of the relative abundance of different classes of proteins in the aggregates isolated from SecE-depleted cells. About 70% of the total band intensity represented secretory proteins, and about 18% represented cytoplasmic proteins, with the cytoplasmic chaperones DnaK and IbpA together constituting 2%.

Effect of SecE depletion on the outer and inner membrane proteomes. To study the effect of SecE depletion on the insertion and composition of the inner and outer membrane proteomes, cells were labeled with [^{35}S]methionine. Outer and inner membranes were subsequently isolated using a combination of a French press and sucrose gradient centrifugation (see Fig. S1 in the supplemental material). The outer membrane proteome was analyzed by 2DE using isoelectric focusing in the first dimension and SDS-PAGE in the second dimension (5). The inner membrane proteome was analyzed with 2D BN/SDS-PAGE with an immobilized first dimension, which allowed reliable comparative analysis of 2D BN/SDS gels (67). Gels were stained with colloidal Coomassie brilliant blue for detection of the steady-state proteome, while [^{35}S]methionine-labeled proteins (i.e., proteins synthesized and inserted during the 1-min pulse and the 10-min chase) were detected by phosphorimaging. As expected, more spots were detected with Coomassie brilliant blue staining than with phosphorimaging. Spot intensities were quantified and compared using PDQuest. Each analysis set contained at least three biological replicates, and statistically significant changes were identified using the Student *t* test and a 95% level of confidence. Interestingly, although quantitative differences were observed, SecE depletion led to qualitatively similar effects on spots detected by Coomassie brilliant blue staining or phosphorimaging. Spots were excised and used for protein identification by MALDI-TOF MS and PMF.

Outer membrane proteome. MS analysis of the Coomassie brilliant blue-stained spots in the 2D gels of the outer membrane proteome resulted in identification of 39 different proteins from 48 spots (Fig. 5A; see Table S3 in the supplemental material). Forty of these spots could be matched with spots detected by phosphorimaging (Fig. 5B). We found that the outer membrane fraction of SecE-depleted cells was contaminated with aggregates that can cosediment with outer membranes during density gradient centrifugation (35, 39). The spots corresponding to aggregated proteins were identified and removed from the analysis set as described in Materials and Methods (see Table S3 and Fig. S4 in the supplemental material).

Figure 5C shows the average changes in the spot intensities (SecE depletion/control) for proteins detected by Coomassie brilliant blue staining and by phosphorimaging. Statistically significant ($P < 0.05$) changes are indicated in Table 3 and in Table S3 in the supplemental material. The steady-state levels and insertion efficiencies of most outer membrane proteins were reduced upon SecE depletion. The levels of three outer membrane proteins, OmpA, Pal, and FadL, were unaffected or slightly increased upon SecE depletion. After the 10-min chase, the level of [^{35}S]methionine-labeled OmpA detected in the outer membrane of SecE-depleted cells was not significantly affected, indicating that translocation of OmpA was slowed but not abolished upon SecE depletion. Furthermore, the steady-state level of OmpA was increased by approximately 20% (Fig. 5A and Table 3; see Table S3 in the supplemental material), which is in keeping with the pulse-chase analysis shown in Fig. 1D.

Inner membrane proteome. MS analysis identified proteins in 76 spots on the Coomassie brilliant blue-stained 2D BN/SDS-PAGE gels. Twenty-one additional spots were annotated with the help of our previously published reference map (Fig. 6A and B and Table 4; see Table S4 in the supplemental material) (67). Fifty-three proteins were integral membrane proteins, and 27 proteins were proteins located at the cytoplasmic side of the inner membrane, mostly as part of membrane-localized complexes. In addition, five secretory proteins were identified in the 2D BN/SDS-PAGE gels.

Figure 6C shows the effect of the SecE depletion expressed as changes calculated from the average spot intensities (SecE depletion/control) of Coomassie brilliant blue-stained and [^{35}S]methionine-labeled proteins. Statistically significant ($P < 0.05$) changes are indicated in Table 4 and in Table S4 in the supplemental material. Since several proteins were identified in more than one spot, we also calculated the effect of SecE depletion on the total level of each identified integral membrane protein (see Table S5 in the supplemental material). This change analysis was used to search for trends among the proteins that appeared to be affected or unaffected upon SecE depletion. The total levels of approximately 30 integral membrane proteins were reduced in the membrane of SecE-depleted cells. Notably, the steady-state levels of all components of the FtsH-HflKC protease complex were significantly reduced (Table 4; see Table S4 in the supplemental material). It is possible that this could affect the stability of the inner membrane proteome, although it should be noted that FtsH-HflKC-

PDQuest. Significantly affected ($P < 0.05$) proteins are indicated in Table 3 and in Table S3 in the supplemental material. (A) Representative 2D gels showing proteins in the outer membrane fraction stained with colloidal Coomassie brilliant blue (protein steady-state levels). (B) Representative 2D gels showing proteins in the outer membrane fraction detected by phosphorimaging (protein insertion). (C) Graph showing the changes (average spot intensity for SecE-depleted samples/average spot intensity for control sample) for proteins visualized by Coomassie brilliant blue staining (black bars) and phosphorimaging (gray bars). A change of 100-fold indicates that a spot was detected only in SecE-depleted samples ("on response"), and a change of 0.01-fold indicates that a spot was detected only in the control samples ("off response"). The numbers correspond to spots on the gels in panels A and B.

TABLE 3. Comparative 2D gel analysis and MS identification of proteins in the outer membrane fraction of SecE-depleted and control cells[a]

Spot[b]	Gene[c]	Swiss-Prot accession no.	Protein							
			Designation or function[d]	Localization or no. of transmembrane segments[e]	Predicted mol wt (10^3) (precursor/mature)[f]	Predicted pI (precursor/mature)[g]	Observed mol wt (10^3)[h]	Observed pI[i]	Coomassie brilliant blue change (fold) (SecE depleted/control)[j]	Phosphorimaging change (fold) (SecE depleted/control)[j]
1	*mdtE*	P37636	Multidrug resistance protein MdtE	im lp	41.3/38.9	5.73/5.12	53.22	4.14	1.06	ND
2	*dcrB*	P0AEE1	DcrB	amb	19.8/17.8	5.09/4.91	17.7	4.29	0.22	0.70
3	*yfgL*	P77774	Lipoprotein YfgL	om lp	41.9/39.9	4.72/4.61	37.75	4.35	0.83	0.76
4	*fhuE*	P16869	FhuE receptor	om	81.2/77.4	4.75/4.72	77.17	4.65	**0.25**	0.56
5	*hemX*	P09127	Putative uroporphyrinogen-III C-methyltransferase	1	42.9	4.68	45.08	4.59	**1.93**	**1.93**
7	*imp*	P31554	Lipopolysaccharide assembly protein	om	89.7/87.1	4.94/4.85	91.39	4.87	0.50	**0.01**
8	*yaeT*	P0A940	Outer membrane protein assembly factor YaeT	om	90.6/88.4	4.93/4.87	88.4	4.87	**0.33**	0.62
12	*fadL*	P10384	Long-chain fatty acid transport protein	om	48.5/45.9	5.09/4.91	44.86	4.84	**1.03**	**1.17**
14	*nlpB*	P0A903	Lipoprotein 34	om lp	36.9/34.4	5.34/4.96	34.68	4.74	**0.52**	1.01
15	*metQ*	P28635	D-Methionine-binding lipoprotein MetQ	om/im lp	29.5/27.2	5.13/4.93	26.94	4.76	**0.07**	ND
16	*tsx*	P0A927	Nucleoside-specific channel-forming protein Tsx	om	33.6/31.4	5.07/4.87	27.47	4.86	0.61	1.25
17	*ybaY*	P77717	Hypothetical lipoprotein YbaY	om/im lp	19.5/17.7	7.88/6.31	23.21	4.78	0.44	ND
19	*mdtE*	P37636	Multidrug resistance protein MdtE	im lp	41.2/38.9	5.73/5.12	40.1	4.97	**0.31**	ND
20	*tsx*	P0A927	Nucleoside-specific channel-forming protein Tsx	om	33.6/31.4	5.07/4.87	27.54	4.96	**0.47**	0.50
21	*mipA*	P0A908	MltA-interacting protein	om	27.8/25.7	5.50/5.03	25.74	4.95	**0.26**	0.64
23	*ompX*	P0A917	Outer membrane protein X	om	18.6/16.4	6.56/5.3	16.12	4.91	0.49	1.13
24	*cirA*	P17315	Colicin I receptor	om	74.1/71.2	5.11/5.03	75.78	5.05	**0.11**	0.77
25	*yiaF*	P0ADK0	Hypothetical protein YiaF	amb	30.43	9.35	23.57	5.01	**0.21**	0.91
26	*fhuA*	P06971	Ferrichrome iron receptor	om	82.4/78.7	5.47/5.13	79.29	5.16	**0.32**	0.77
27	*btuB*	P06129	Vitamin B_{12} transporter BtuB	om	68.4/66.3	5.23/5.10	66.13	5.13	**0.48**	1.02
28	*tolC*	P02930	Outer membrane protein TolC	om	53.7/51.5	5.46/5.23	52.68	5.13	**0.50**	0.78
29	*nlpA*	P04846	Lipoprotein 28	im lp	29.4/27.1	5.77/5.29	26.64	5.12	**0.23**	0.01
30	*mipA*	P0A908	MltA-interacting protein	om	27.8/25.7	5.50/5.03	25.52	5.11	**0.49**	1.02
32	*pal*	P0A912	Peptidoglycan-associated lipoprotein	om lp	16.9/16.6	6.29/5.59	17.65	5.08	**1.02**	1.14
33	*fepA*	P05825	Ferrienterobactin receptor	om	82.1/79.8	5.39/5.23	81.97	5.23	**0.07**	0.43
34	*yfiO*	P0AC02	Lipoprotein YfiO	om lp	27.9/25.8	6.16/5.48	24.87	5.2	**0.59**	0.62
35	*ompX*	P0A917	Outer membrane protein X	om	18.6/16.4	6.56/5.3	15.7	5.25	**0.64**	**0.72**
36	*pal*	P0A912	Peptidoglycan-associated lipoprotein	om lp	16.9/16.6	6.29/5.59	17.43	5.38	**1.19**	**1.12**
41	*yfiO*	P0AC02	Lipoprotein YfiO	om lp	27.9/25.8	6.16/5.48	25.39	5.53	**0.69**	**ND**
42	*ompW*	P0A915	Outer membrane protein W	om	22.9/20.9	6.03/5.58	21.5	5.54	**0.31**	**0.10**
43	*fusA*	P0A6M8	Elongation factor G	c	77.6	5.24	83.22	5.69	**0.09**	ND
44	*yicH*	P31433	Hypothetical protein YicH	sec	62.3/58.7	5.67/5.38	63.8	5.85	0.15	ND
45	*ompA*	P0A910	Outer membrane protein A	om	37.2/35.2	5.99/5.60	31.74	6	**1.22**	1.12
48	*ompX*	P0A917	Outer membrane protein X	om	18.6/16.4	6.56/5.3	16.49	6.19	**0.37**	**0.46**

[a] The spots in 2D gels of the outer membrane fraction from SecE-depleted and control cells were excised from gels stained with colloidal Coomassie brilliant blue (Fig. 5A). Proteins were identified by MALDI-TOF MS and PMF. Spots visualized by Coomassie brilliant blue staining and phosphorimaging (Fig. 5A and B) were quantified and compared using PDQuest. Quantities of Coomassie brilliant blue-stained spots were normalized using the "total quantity of valid spot" tool, excluding spots detected in the 2D gels of protein aggregates extracted from the outer membrane fraction (see Fig. S1 in the supplemental material). Quantities of spots visualized by phosphorimaging were normalized using the normalization factor calculated for the corresponding Coomassie brilliant blue-stained gel. Changes of 0.01- and 100-fold correspond to spots that are missing ("off response") and spots that are turned on ("on response") in the SecE-depleted cells, respectively. Significant changes ($P < 0.05$) are indicated by bold type. Graphs of changes are shown in Fig. 5C.

[b] The numbers correspond to the spot numbers in the 2D gels shown in Fig. 5A and B.

[c] Gene designations in the Swiss-Prot database for *E. coli*.

[d] Protein designations in the Swiss-Prot database for *E. coli*.

[e] Localization based on the information given in the Swiss-Prot database for *E. coli*. Unknown localizations were predicted by PSORT (http://psort.hgc.jp/form.html). Abbreviations: amb, ambiguous; c, cytoplasmic; im lp, inner membrane lipoprotein; om, outer membrane; om lp, outer membrane lipoprotein; sec, secretory.

[f] Protein sizes predicted from amino acid sequences. Two sizes are given for secretory proteins; the first size is the size of the precursor form including the signal sequence, and the second size is the size of the mature form of the protein after signal sequence processing.

[g] pIs predicted from amino acid sequences. Two values are given for secretory proteins; the first value is the pI for the precursor form, and the second value is the pI for the mature form of the protein.

[h] Sizes of proteins calculated from the spot positions on the 2D gels shown in Fig. 5.

[i] pIs of proteins calculated from the spot positions on the 2D gels shown in Fig. 5.

[j] Changes expressed as the ratio of the average spot intensities. ND, not determined.

mediated proteolysis has been shown for only a few membrane proteins (32). The levels of the cytochrome bo_3 terminal oxidase subunits CyoA and CyoB were reduced by 75 and 85%, respectively. The biogenesis of CyoA, which is a lipid-modified integral membrane protein, has recently been shown to depend on both YidC and the Sec translocon (12, 20, 62).

Interestingly, the total levels of a surprisingly large number of integral membrane proteins (approximately 30 proteins) seemed to be hardly affected or even increased by SecE depletion (see Table S5 in the supplemental material). The total levels of the following proteins appeared to be increased in the inner membrane of SecE-depleted cells: Aas, AtpF, MscS, MgtA, YbbK, YhcB, YhjG, and YajC. We tested if the effect of SecE depletion could be correlated to different membrane protein properties. Protein abundance, topology, hydrophobicity, and the energy required for membrane integration of the first transmembrane domain (30) did not correlate with the effect on total protein levels upon SecE depletion (data not shown). However, when the changes (Coomassie brilliant blue staining) were plotted against the number of amino acids in the largest translocated domain of each protein, we found that almost all proteins with large periplasmic domains are sensitive to SecE depletion (Fig. 7A; see Table S5 in the supplemental material). In contrast, almost all proteins that were positively affected by SecE depletion do not contain any large periplasmic domain. A closer look at the proteins that were identified in spots that did not follow this trend (Aas, YhjG, YbbK, and YhcB) revealed that they consist of only one or two transmembrane segments. This prompted us to perform a combined analysis of the effect of the number of transmembrane segments and the size of periplasmic domains. Based on the plot shown in Fig. 7A, we divided the proteins into two groups: proteins with large translocated domains ($\geq$60 amino acids) and proteins with small translocated domains ($\leq$60 amino acids). The 60-amino-acid cutoff for Sec dependence is in agreement with previous studies (3). The effect of SecE depletion on these two groups was plotted against the number of transmembrane segments (Fig. 7B; see Table S5 in the supplemental material). This analysis clearly demonstrated that proteins that do not have large periplasmic domains are overrepresented among the proteins that are either unaffected ($\geq$0.75-fold and $\leq$1.25-fold change) or positively affected ($\geq$1.25-fold change) by SecE depletion. The few exceptions are proteins that contain only one or two transmembrane segments. Collectively, our analysis suggests that many proteins that lack large periplasmic domains and/or contain one or two transmembrane segments can insert efficiently into the membrane when the levels of the Sec translocon are strongly reduced.

DISCUSSION

So far, the role of the Sec translocon in protein translocation and insertion in *E. coli* has been studied using focused approaches and a very limited set of model substrates. Therefore, we studied protein translocation and insertion in *E. coli* cells depleted of the essential translocon component SecE and control cells using comparative proteomics. Depletion of SecE resulted in a 90% (10-fold) reduction in the level of SecE, while the levels of SecY and SecG were reduced by 50 and 20%, respectively. 1D BN-PAGE combined with immunoblotting showed that the level of the SecYEG complex was strongly reduced upon SecE depletion. Furthermore, the accumulation level of SecA was increased 1.7-fold. This indicates that translocation of the translocation monitor SecM is hampered due to insufficient Sec translocon capacity, leading to increased expression of SecA (44). SecE depletion did not affect the accumulation levels of SecB and Ffh, both of which are involved in protein targeting.

Our analysis of the subproteomes of cells with strongly reduced Sec translocon levels resulted in three main observations and conclusions. Reduced Sec translocon levels (i) resulted in the accumulation of secretory proteins in the cytoplasm, the formation of protein aggregates, and a σ^{32} response, (ii) negatively affected levels of all constituents of the outer membrane proteome with the exception of OmpA, Pal, and FadL, and (iii) appeared to differentially affect inner membrane proteins (the steady-state levels and insertion of some integral inner membrane proteins were reduced, while the levels of other proteins were not affected or even increased in the membranes of SecE-depleted cells). Our analysis indicates that proteins whose levels were unaffected or increased upon SecE depletion lack large translocated domains and/or consist of only one or two transmembrane segments. Below, these main observations and conclusions are explained and discussed in more detail.

Reduced Sec translocon levels induce the formation of protein aggregates. Upon SecE depletion, secretory proteins accumulate in the cytoplasm, leading to aggregate formation and the induction of a σ^{32} response. It was estimated that secretory proteins made up 70% of the total protein in the aggregates. The MS/MS analysis revealed that at least three secretory proteins, OmpA, Lpp, and β-lactamase, contained an uncleaved signal sequence, pointing to aggregation in the cytoplasm rather than in the periplasm. Sequence analysis of all the aggregated secretory proteins with the aggregation propensity prediction program Tango showed that their signal sequences are more aggregation prone than the mature parts of the proteins (23; data not shown). This suggests that secretory proteins are more prone to aggregation in the cytoplasm than in the periplasm. The accumulation of secretory proteins upon SecE depletion induced a σ^{32} response, leading to increased levels of the cytoplasmic chaperones IbpA/B, DnaK, GroEL, and ClpB. These chaperones protect proteins from aggregation and are also involved in the disaggregation, refolding, and degradation of aggregated proteins (10, 11, 68). IbpA/B, DnaK, DnaJ, and GroEL were among the proteins that were identified in the aggregate fraction. Thus, aggregated secretory proteins may be either actively reactivated for translocation or degraded. Recently, we have shown that OmpA can be extracted from cytoplasmic aggregates of an *E. coli secB* null mutant (5). Although our analysis did not provide any evidence for aggregate formation in the periplasm of SecE-depleted cells, we cannot exclude this possibility.

Only a few inner membrane proteins were identified in the aggregates. This may be explained by the efficient degradation by SsrA mRNA-dependent tagging of stalled nascent chains of cotranslationally targeted membrane proteins and subsequent turnover by proteases (14, 69). Sec translocon-independent membrane insertion mechanisms could also explain the low abundance of inner membrane proteins in the aggregates (see below).

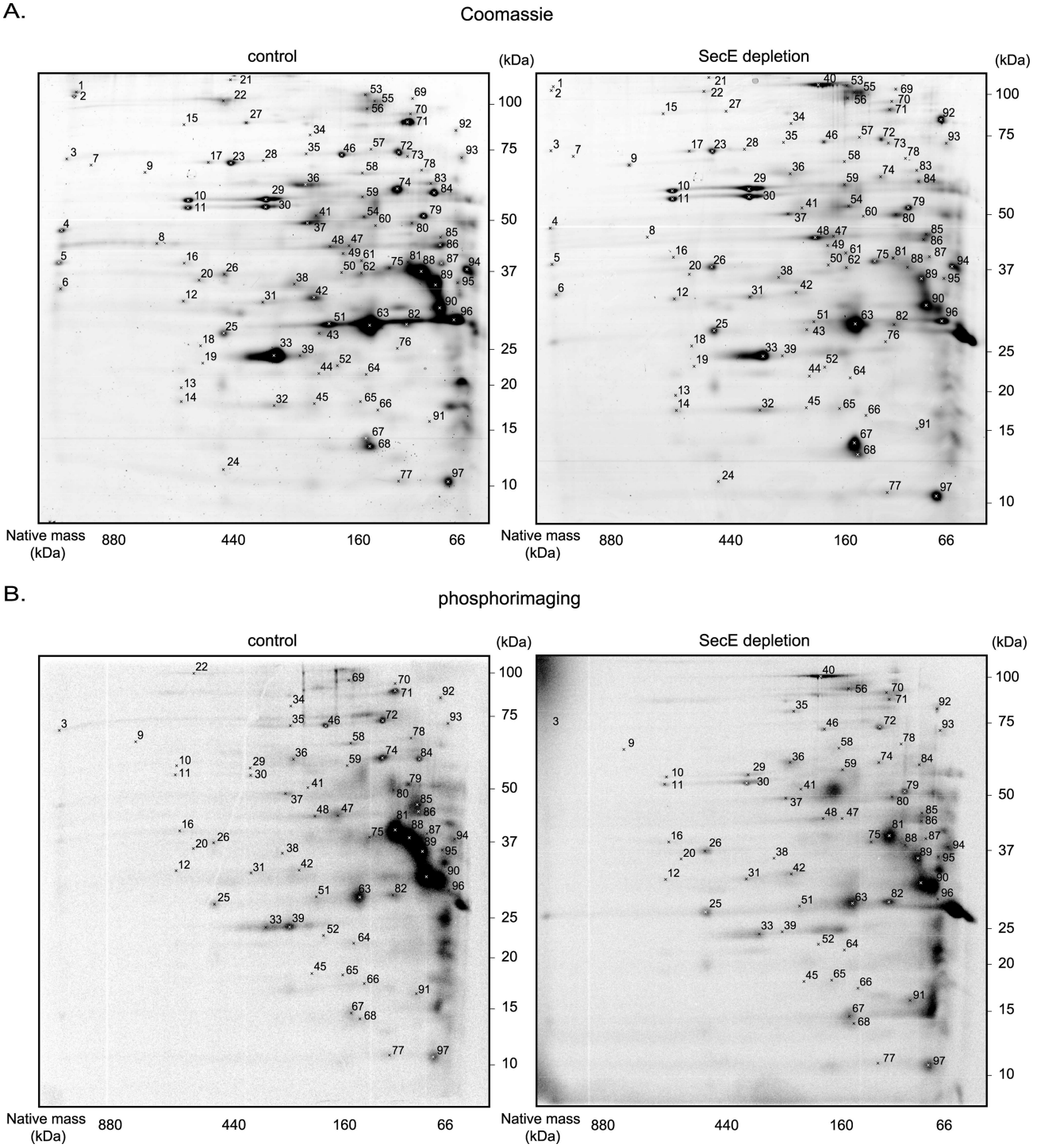

FIG. 6. 2D BN/SDS-PAGE analysis of the inner membrane proteomes of SecE-depleted and control cells. Cells were labeled with [^{35}S]methionine for 1 min, which was followed by a chase for 10 min with cold methionine. The inner membrane fractions were isolated by density centrifugation from a mixture of labeled and nonlabeled cells as outlined in Fig. S1 in the supplemental material (see Materials and Methods for details). The inner membrane fractions were analyzed by 2D BN/SDS-PAGE. Proteins were identified by MALDI-TOF MS and PMF (Table 4; see Table S4 in the supplemental material) using spots excised from Coomassie brilliant blue-stained gels. If several proteins were identified in one spot, the first gene listed corresponds to the protein with the highest Mascot MOWSE score. Primary gene designations were obtained from Swiss-Prot (www.expasy.org). Differences in the inner membrane proteomes of SecE-depleted and control cells were analyzed using PDQuest. Significantly affected ($P < 0.05$) proteins are indicated in Table 4 and in Table S4 in the supplemental material. (A) Representative 2D BN/SDS-PAGE gels with proteins detected by staining with colloidal Coomassie brilliant blue (protein steady-state levels). (B) Representative 2D BN/SDS-PAGE gels with proteins detected by phosphorimaging (protein insertion). (C) Graph showing the changes (average spot intensities for SecE-depleted samples/average spot intensities for control samples) for proteins detected by Coomassie brilliant blue staining (black bars) and phosphorimaging (gray bars). A change of 100-fold indicates a spot that was detected only in SecE-depleted samples ("on response"), and a change of 0.01-fold indicates that a spot was detected only in the control samples ("off response"). The numbers correspond to spots on the gels in panels A and B.

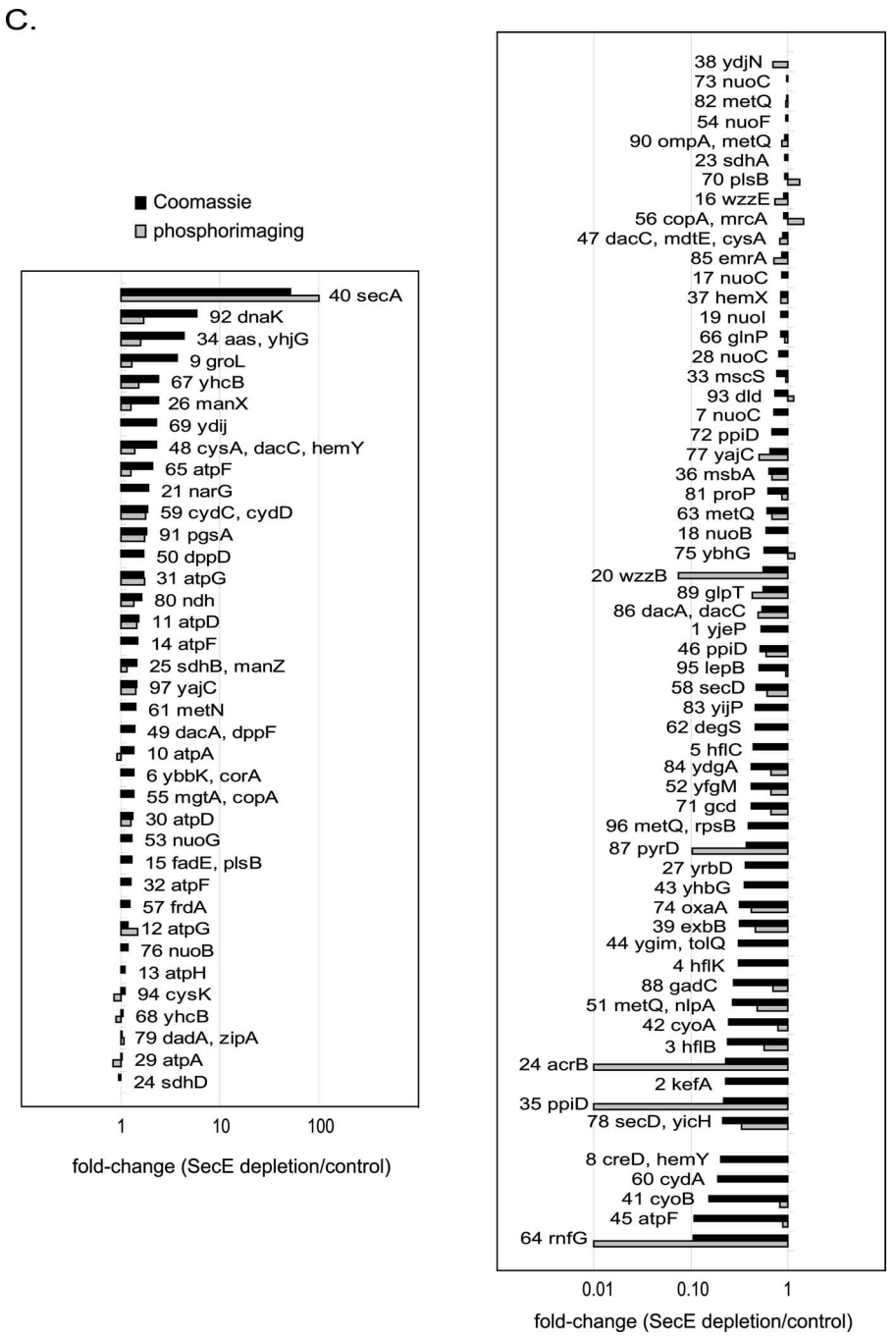

FIG. 6—*Continued*.

SecE depletion reduces the insertion and steady-state levels of most outer membrane proteins. A direct correlation between the effects on the outer membrane proteome and Sec translocon dependence is difficult to make since key players involved in outer membrane protein biogenesis, like YaeT and Skp (56), are affected by SecE depletion. Nevertheless, analysis of the outer membrane proteome indicated that translocation of proteins across the inner membrane is hampered but not blocked upon SecE depletion. The components of the outer membrane proteome were differentially affected by the depletion of SecE. The levels of OmpA, FadL, and Pal were unaffected or increased in the outer membrane upon SecE depletion, while the levels of most other outer membrane proteins were reduced to different extents. One possible explanation for this is superior access of these proteins to the Sec translocons still present upon SecE depletion. Signal peptide-based selective modulation of protein translocation occurs in the endoplasmic reticulum during stress (33). If such a mechanism for modulation of translocation efficiency exists in *E. coli*, it should become apparent when Sec translocon levels are lowered. We

TABLE 4. 2D BN/SDS-PAGE analysis of the inner membrane proteome of SecE-depleted and control cells[a]

Spot[b]	Gene[c]	Protein: Designation or function[d]	Localization or no. of transmembrane segments[e]	Predicted mol wt (10^3) (precursor/mature)[f]	Observed mol wt (10^3)[g]	Observed native mol wt (10^3)[h]	Coomassie brilliant blue change (fold) (SecE depleted/control)[i]	Phosphorimaging change (fold) (SecE depleted/control)[i]
1	*yjeP*	Hypothetical MscS family protein YjeP	10	124.0	103.7	1,000	0.52	ND
2	*kefA*	Potassium efflux system KefA	11	127.2	100.7	1,000	0.23	ND
3	*ftsH*	Cell division protease FtsH	2	70.7	69.3	1,000	**0.24**	0.56
4	*hflK*	HflK	1	45.5	45.4	1,000	0.31	ND
5	*hflC*	HflC	1	37.7	37.4	1,000	0.43	ND
6	*ybbK*	Hypothetical protein YbbK	1	33.7	32.2	1,000	1.36	ND
6	*corA*	Magnesium transport protein CorA	2	36.6	32.2	1,000	1.36	ND
7	*nuoC*	NADH-quinone oxidoreductase subunit C/D	c, im ass	68.7	67.1	966	0.70	ND
8	*creD*	Inner membrane protein CreD	6	49.8	42.7	733	**0.20**	ND
8	*hemY*	HemY	2	45.2	42.7	733	**0.20**	ND
9	*groL*	60-kDa chaperonin	c	57.2	64.0	828	**3.72**	1.30
10	*atpA*	ATP synthase subunit alpha	c, im ass	55.2	55.4	638	1.36	0.91
11	*atpD*	ATP synthase subunit beta	c, im ass	50.2	53.0	637	1.50	1.44
12	*atpG*	ATP synthase gamma chain	c, im ass	31.6	31.4	614	1.19	1.49
13	*atpH*	ATP synthase delta chain	c, im ass	19.3	20.8	606	1.11	ND
14	*atpF*	ATP synthase B chain	1	17.3	18.9	599	1.47	ND
15	*fadE*	Acyl-coenzyme A dehydrogenase	2	89.2	85.1	600	1.28	ND
15	*plsB*	Glycerol-3-phosphate acyltransferase	c, im ass	91.3	85.1	600	1.28	ND
16	*wzzE*	Lipopolysaccharide biosynthesis protein WzzE	2	39.6	38.6	603	0.90	0.72
17	*nuoC*	NADH-quinone oxidoreductase subunit C/D	c, im ass	68.7	68.1	543	0.86	ND
18	*nuoB*	NADH-quinone oxidoreductase subunit B	c, im ass	25.1	25.5	510	**0.59**	ND
19	*nuoI*	NADH-quinone oxidoreductase subunit I	c, im ass	20.5	23.5	509	0.84	ND
20	*wzzB*	Chain length determinant protein	2	36.5	35.1	531	0.55	0.07
21	*narG*	Respiratory nitrate reductase 1 alpha chain	c, im ass	140.4	113.1	463	1.92	ND
22	*acrB*	Lavine resistance protein B	12	113.6	92.7	478	**0.23**	**0.01**
23	*sdhA*	Succinate dehydrogenase flavoprotein subunit	c, im ass	64.4	68.6	440	0.92	ND
24	*sdhD*	Succinate dehydrogenase hydrophobic membrane anchor subunit	4	12.9	12.0	427	0.94	ND
25	*sdhB*	Succinate dehydrogenase iron-sulfur subunit	c, im ass	26.8	27.2	438	1.44	1.14
25	*manZ*	Mannose permease IID component	1	31.3	27.2	438	1.44	1.14
26	*manX*	Phosphotransferase system mannose-specific EIIAB component	c, im ass	34.9	36.8	439	**2.40**	1.26
27	*yrbD*	Hypothetical protein YrbD	sec	19.6/16.5	87.5	426	**0.36**	ND
28	*nuoC*	NADH-quinone oxidoreductase subunit C/D	c, im ass	68.7	69.3	363	0.81	ND
29	*atpA*	ATP synthase subunit alpha	c, im ass	55.2	56.4	366	1.02	0.83
30	*atpD*	ATP synthase subunit beta	c, im ass	50.2	54.0	364	1.33	1.26
31	*atpG*	ATP synthase gamma chain	c, im ass	31.6	32.2	348	**1.68**	1.73
32	*atpF*	ATP synthase B chain	1	17.3	19.5	301	1.27	ND
33	*mscS*	Small-conductance mechanosensitive channel	3	30.9	24.4	302	0.77	0.94
34	*aas*	AAS bifunctional protein	2	80.7	78.7	248	**4.38**	1.59
34	*yhjG*	Hypothetical protein YhjG	2	75.1	78.7	248	**4.38**	1.59
35	*ppiD*	Peptidyl-prolyl *cis-trans* isomerase D	1	68.2	71.6	264	**0.22**	**0.01**
36	*msbA*	Lipid A export ATP-binding/permease protein MsbA	5	64.5	59.7	238	0.64	0.68
37	*hemX*	Putative uroporphyrinogen-III C-methyltransferase	1	43.0	49.0	265	0.84	0.83
38	*ydjN*	Hypothetical symporter YdjN	9	48.7	35.1	272	0.98	0.69
39	*exbB*	Biopolymer transport ExbB protein	3	26.3	24.7	243	**0.31**	**0.46**
40	*secA*	Preprotein translocase subunit SecA	c, im ass	102.0	108.1	209	**50.77**	**100.00**
41	*cyoB*	Ubiquinol oxidase subunit 1	15	74.4	50.7	203	**0.15**	0.81
42	*cyoA*	Ubiquinol oxidase subunit 2	2	34.9	32.6	201	**0.25**	0.79
43	*yhbG*	Probable ABC transporter ATP-binding protein YhbG	c, im ass	26.7	27.5	201	**0.35**	ND
44	*ygiM*	Hypothetical protein YgiM	1	23.1	22.6	218	**0.31**	ND
44	*tolQ*	TolQ	3	25.6	22.6	218	**0.31**	ND
45	*atpF*	ATP synthase B chain	1	17.3	20.1	200	**0.11**	0.88
46	*ppiD*	Peptidyl-prolyl *cis-trans* isomerase D	1	68.2	71.4	176	**0.51**	0.59
47	*dacC*	Penicillin-binding protein 6	1*	43.6/40.8	42.6	158	0.87	0.81
47	*mdtE*	Multidrug resistance protein MdtE	im, lp	41.2	42.6	158	0.87	0.81
47	*cysA*	Sulfate/thiosulfate import ATP-binding protein CysA	c, im ass	41.1	42.6	158	0.87	0.81
48	*cysA*	Sulfate/thiosulfate import ATP-binding protein CysA	c, im ass	41.1	43.1	177	**2.27**	1.37
48	*dacC*	Penicillin-binding protein 6	1*	41.1	43.1	177	**2.27**	1.37
48	*hemY*	HemY	2	45.2	43.1	177	2.27	1.37
49	*dacA*	Penicillin-binding protein 5	1*	44.4/41.3	41.4		1.40	ND
49	*dppF*	Dipeptide transport ATP-binding protein DppF	c, im ass	37.6	41.4	160	1.40	ND
50	*dppD*	Dipeptide transport ATP-binding protein DppD	c, im ass	35.8	37.3	160	1.70	ND
51	*metQ*	D-Methionine-binding lipoprotein MetQ	im/om lp	29.4/27.2	29.0	166	**0.27**	**0.48**
51	*nlpA*	Lipoprotein 28	im/om lp	29.4/27.1	29.0	166	**0.27**	**0.48**
52	*yfgM*	YfgM	1	22.2	23.7	165	**0.41**	0.66
53	*nuoG*	NADH-quinone oxidoreductase subunit F	c, im ass	100.2	102.5	159	1.30	ND
54	*nuoF*	NADH-quinone oxidoreductase subunit G	c, im ass	49.3	51.1	150	0.95	ND
55	*mgtA*	Magnesium-transporting ATPase, P-type 1	10	99.5	98.6	149	**1.34**	ND
56	*copA*	Copper-transporting P-type ATPase	8	87.7	93.4	158	0.90	1.44
56	*mrcA*	Penicillin-binding protein 1A	1	93.6	93.4	158	0.90	1.44
57	*frdA*	Fumarate reductase flavoprotein subunit	c, im ass	65.8	74.2	145	1.24	ND

Continued on following page

TABLE 4—*Continued*

Spot[b]	Gene[c]	Protein: Designation or function[d]	Localization or no. of transmembrane segments[e]	Predicted mol wt (10^3) (precursor/mature)[f]	Observed mol wt (10^3)[g]	Observed native mol wt (10^3)[h]	Coomassie brilliant blue change (fold) (SecE depleted/control)[i]	Phosphorimaging change (fold) (SecE depleted/control)[i]
58	*secD*	Protein-export membrane protein SecD	6	66.6	65.5	151	**0.47**	**0.60**
59	*cydC*	Transport ATP-binding protein CydC	6	62.9	57.5	150	1.86	1.79
59	*cydD*	Transport ATP-binding protein CydD	6	65.1	57.5	150	1.86	1.79
60	*cydA*	Cytochrome *d* ubiquinol oxidase subunit 1	7	58.2	48.1	137	**0.19**	ND
61	*metN*	Methionine import ATP-binding protein MetN	c	37.8	40.4	147	**1.41**	ND
62	*degS*	Protease DegS	p	37.6/34.6	37.7	151	**0.45**	ND
63	*metQ*	D-Methionine-binding lipoprotein MetQ	im/om lp	29.4/27.2	29.1	135	**0.61**	0.67
64	*rnfG*	Electron transport complex protein RnfG	1	21.9	22.6	143	**0.10**	**0.01**
65	*atpF*	ATP synthase B chain	1	17.3	20.1	149	**2.07**	1.25
66	*glnP*	Glutamine transport system permease protein GlnP	5	24.4	19.0	128	0.83	0.92
67	*yhcB*	Putative cytochrome *d* ubiquinol oxidase subunit III	1	15.2	14.5	144	**2.41**	1.52
68	*yhcB*	Putative cytochrome *d* ubiquinol oxidase subunit III	1	15.2	14.6	133	1.05	0.90
69	*ydiJ*	Hypothetical protein YdiJ	amb	113.2	103.2	115	**2.27**	ND
70	*plsB*	Glycerol-3-phosphate acyltransferase	c, im ass	91.3	94.4	116	0.91	*1.31*
71	*gcd*	Quinoprotein glucose dehydrogenase	5	86.7	89.7	117	**0.41**	0.66
72	*ppiD*	Peptidyl-prolyl *cis-trans* isomerase D	1	68.2	73.1	126	0.68	0.99
73	*nuoC*	NADH-quinone oxidoreductase subunit C/D	c, im ass	68.7	72.2	119	0.96	ND
74	*oxaA*	Inner membrane protein OxaA	6	61.5	60.6	125	**0.31**	**0.42**
75	*ybhG*	Membrane protein YbhG	1	36.4/34.4	37.9	130	0.56	1.17
76	*nuoB*	NADH-quinone oxidoreductase subunit B	c, im ass	25.1	26.5	119	1.17	ND
77	*yajC*	Membrane protein YajC	1	11.9	11.7	111	0.65	**0.51**
78	*secD*	Protein export membrane protein SecD	6	66.6	67.5	106	**0.21**	0.33
78	*yicH*	Hypothetical protein YicH	amb	62.3	67.5	106	**0.21**	**0.33**
79	*dadA*	D-Amino acid dehydrogenase small subunit	c, im ass	47.6	52.2	105	1.04	1.07
79	*zip*	Cell division protein ZipA	1	36.5	52.2	105	1.04	1.07
80	*ndh*	NADH dehydrogenase	amb	47.2	49.3	111	**1.63**	1.36
81	*proP*	Proline/betaine transporter	12	54.8	41.7	111	0.62	0.85
82	*metQ*	D-Methionine-binding lipoprotein MetQ	im/om lp	29.4/27.2	29.1	110	0.96	0.94
83	*yijP*	Membrane protein YijP	5	66.6	62.9	96	**0.45**	ND
84	*ydgA*	Protein YdgA	p, im ass	54.7/52.8	59.3	96	**0.42**	0.66
85	*emrA*	Multidrug resistance protein A	1	42.7	45.5	89	0.86	0.72
86	*dacA*	Penicillin-binding protein 5	1*	44.4/41.3	43.6	92	**0.53**	0.49
86	*dacC*	Penicillin-binding protein 6	1*	43.6/40.8	43.6	92	**0.53**	0.49
87	*pyrD*	Dihydroorotate dehydrogenase	c, im ass	36.8	39.4	83	**0.37**	**0.10**
88	*gadC*	Probable glutamate/gamma-aminobutyrate antiporter	12	55.1	38.3	98	**0.27**	0.70
89	*glpT*	Glycerol-3-phosphate transporter	12	47.2	50.3	87	**0.54**	**0.42**
90	*ompA*	Outer membrane protein A	om	37.2	31.8	87	0.93	0.87
90	*metQ*	D-Methionine-binding lipoprotein MetQ	im/om lp	29.4/27.2	31.8	87	0.93	0.87
91	*pgsA*	CDP-diacylglycerol–glycerol-3-phosphate 3-phosphatidyltransferase	4	20.6	17.2	86	1.83	1.73
92	*dnaK*	Chaperone protein DnaK	c	69.0	83.7	77	**5.89**	1.72
93	*dld*	D-Lactate dehydrogenase	c, im ass	64.5	73.3	71	**0.72**	1.15
94	*cysK*	Cysteine synthase A	c	34.4	38.1	63	1.10	0.86
95	*lepB*	Signal peptidase I	2	36.0	35.2	69	0.50	0.95
96	*metQ*	D-Methionine-binding lipoprotein MetQ	im/om lp	29.4/27.2	29.5	70	**0.39**	ND
96	*rpsB*	30S ribosomal protein S2	c	26.6	29.5	70	**0.39**	ND
97	*yajC*	Membrane protein YajC	1	11.9	11.7	71	1.44	1.43

[a] Spots in 2D BN/SDS-PAGE gels of inner membranes (Fig. 6A) were excised from gels stained with colloidal Coomassie brilliant blue. Proteins were identified by MALDI-TOF MS and PMF. The proteins encoded by the following genes belonged to the same complex: *ftsH*, *hflK*, and *hflC* (spots 3 to 5); *atpA*, *atpD*, *atpG*, *atpH*, and *atpF* (spots 10 to 14); *nuoC*, *nuoB*, and *nuoI* (spots 17 to 19); *sdhA*, *sdhD*, and *sdhB* (spots 23 to 25); *manZ* and *manX* (spots 25 and 26); *atpA*, *atpD*, *atpG*, and *atpF* (spots 29 to 32); *cyoB* and *cyoA* (spots 41 and 42); *dppF* and *dppD* (spots 49 and 50); *nuoG* and *nuoF* (spots 53 and 54); and *cydC* and *cydD* (spot 59). Spots visualized by Coomassie brilliant blue staining and/or phosphorimaging (Fig. 6A and B) were quantified and compared using PDQuest. Changes of 0.01- and 100-fold correspond to spots that are missing ("off response") and spots that are turned on ("on response") in the SecE-depleted cells, respectively. Significant changes ($P < 0.05$) are indicated by bold type.

[b] The numbers correspond to the spots in the 2D BN/SDS-PAGE gels shown in Fig. 6A.

[c] Gene designations in the Swiss-Prot database for *E. coli*.

[d] Protein designations in the Swiss-Prot database for *E. coli*.

[e] Localization based on the information given in the Swiss-Prot database for *E. coli.* Unknown localizations were predicted by PSORT. For integral membrane proteins, the number of transmembrane segments is indicated. An asterisk indicates that the membrane-inserted segment may act as an anchor rather than as a true transmembrane segment. Abbreviations: amb, ambiguous; c, cytoplasmic; im ass, inner membrane associated; im lp, inner membrane lipoprotein; om, outer membrane; om lp, outer membrane lipoprotein; sec, secretory.

[f] Protein sizes predicted from amino acid sequences. Two sizes are given for secretory proteins; the first size is the size of the precursor form, and the second size is the size of the mature form of the protein.

[g] Sizes of proteins calculated from the spot positions on the 2D BN/SDS-PAGE gels used for the analysis.

[h] Native molecular weights based on the positions in the 2D BN/SDS-PAGE gel in Fig. 6A.

[i] Changes expressed as the ratio of the average intensity of spots in gels of the SecE-depleted cells to the average intensity of matched spots in the control gels. ND, not determined.

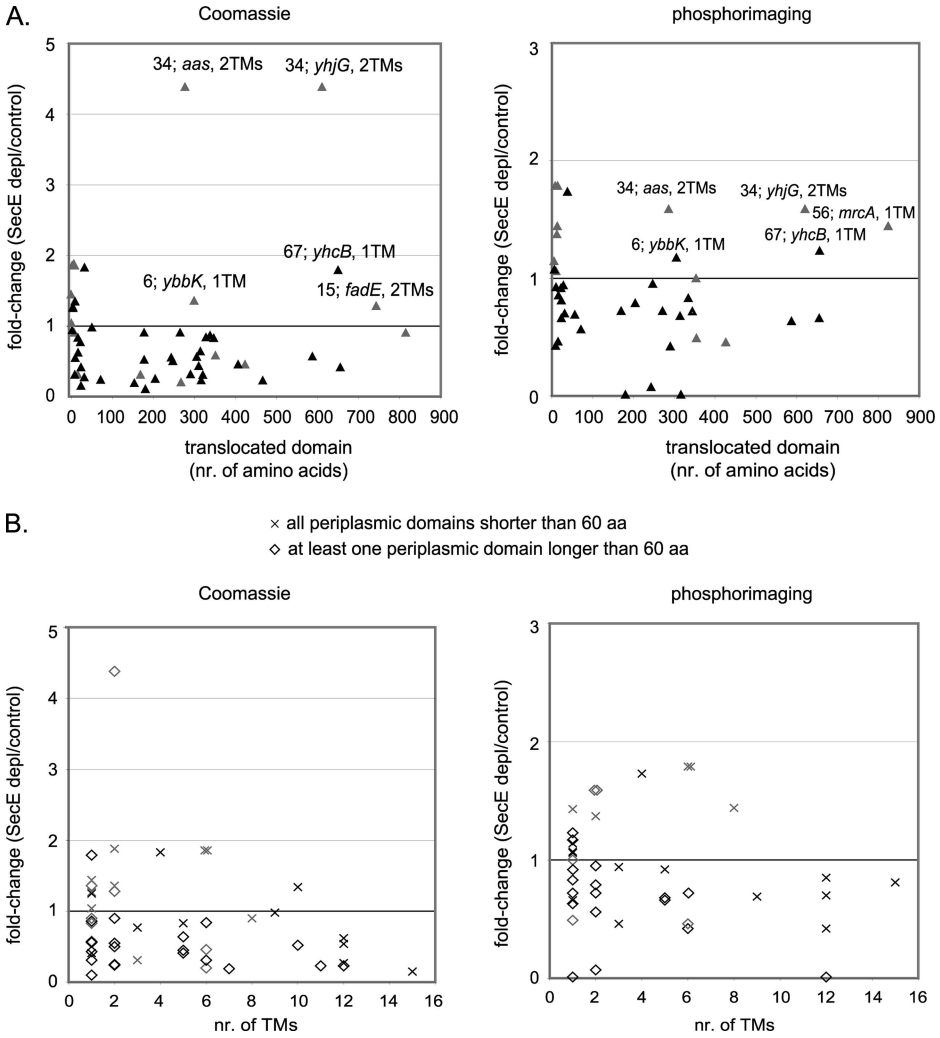

FIG. 7. Correlations between properties of inner membrane proteins and the effect on their steady-state levels and insertion upon SecE depletion. (A) Changes in steady-state levels (Coomassie brilliant blue staining) and insertion (phosphorimaging) plotted against the number of amino acids in the largest translocated domain of each protein (see Table S5 in the supplemental material). Black symbols represent proteins identified in spots containing only one protein, while gray symbols represent proteins identified in spots containing more than one protein. Almost all proteins that appeared to be positively affected by SecE depletion do not contain any large periplasmic domains. Exceptions to this trend are indicated on the plots by gene designations and the number of predicted transmembrane segments (TMs). SecE depl, SecE-depleted cells; aa, amino acids. (B) Proteins were divided into two groups: proteins with large translocated domains (≥60 amino acids) and proteins with small translocated domains (≤60 amino acids). The changes upon SecE depletion for these two groups were plotted against the number of transmembrane segments (see Table S5 in the supplemental material). Black symbols represent proteins identified in spots containing only one protein, while gray symbols represent proteins identified in spots containing more than one protein.

were not able to identify any signal sequence characteristics (e.g., hydrophobicity, charge distribution, or length) that correlated with the differential effects on the constituents of the outer membrane proteome upon depletion of SecE (data not shown).

Using a small number of model proteins, it has been shown that DnaK can keep outer membrane proteins, but not periplasmic proteins, in a prolonged export-competent state upon depletion of SecA (52). This suggests that affinity toward DnaK and other chaperones could also affect the translocation efficiency of secretory proteins during SecE depletion. However, it should be noted that both periplasmic and outer membrane proteins were identified in aggregates from SecE-depleted cells (Fig. 4 and Table 2). We were not able to extend our analysis to include the periplasmic proteome, since it was not possible to isolate sufficiently pure periplasmic fractions from SecE-depleted cells. Thus, it is not clear if the outer membrane proteome is in fact less affected than the periplasmic proteome or if the chaperone-mediated protection of secretory proteins is independent of the final destination of the protein.

It is conceivable that proteins which under normal conditions use the Sec translocon can cross the membrane via alternative pathways upon SecE depletion. It has been shown that a considerable number of *E. coli* TAT signal peptides can mediate the translocation of reporter proteins across the inner membrane via the Sec pathway when the TAT pathway is compromised (61). This suggests that secretory proteins can be

promiscuous, i.e., can use both the the Sec and TAT protein translocation pathways. In this respect it should be noted that the TAT pathway is still operational upon SecE depletion (15). Interestingly, our 2D BN/SDS-PAGE analysis revealed that SecA dimers accumulated at the inner membrane of SecE-depleted cells. Impaired Sec translocon function results in increased expression of SecA, mediated by the secretion monitor SecM (44). SecA is the peripheral subunit of the Sec translocon and is responsible for the ATP-dependent translocation of secretory proteins and large periplasmic domains of integral membrane proteins. The increased levels of SecA may enhance translocation efficiency when the pressure on the translocon is particularly high. Recently, it has been shown that the Sec translocon catalyzes the monomerization of the SecA dimer (2). This could explain the accumulation of SecA dimers at the membrane observed upon SecE depletion. It has also been proposed that the SecA dimer by itself can act as an alternative translocase for secretory proteins (13). If this is indeed the case, it could mean that the SecA dimer functions as a backup translocon when Sec translocon capacity is not sufficient.

SecE depletion has differential effects on the inner membrane proteome. Depletion of SecE resulted in reduced steady-state levels and integration of approximately 30 integral membrane proteins, while the levels of almost as many proteins were not significantly affected or even increased. The immunoblot and 2D BN/SDS-PAGE analysis showed that the levels of FtsQ, Lep, and the cytochrome bo_3 subunit CyoA were all strongly reduced in the inner membrane of SecE-depleted cells. These proteins have been shown to require both the Sec translocon and YidC for proper assembly into the inner membrane (16, 20, 21, 62).

The levels of a surprisingly large number of inner membrane proteins appeared to be either unaffected or even increased in the membrane of SecE-depleted cells. Among the unaffected proteins was the F_oc subunit of the F_o sector of the ATP synthase. This is in keeping with previous studies showing that F_oc is inserted into the inner membrane in a Sec translocon-independent but YidC-dependent fashion (63, 66, 72). The efficient insertion of F_oc demonstrates that the YidC pathway was operational, although the YidC levels were reduced 50% upon SecE depletion. Interestingly, the levels of F_oa and F_ob, which are also components of the F_o sector of the ATP synthase, were slightly increased upon SecE depletion (Table 4 and Fig. 1C, respectively). It has been proposed that insertion of both F_oa and F_ob is dependent on the Sec translocon (72). However, it should be noted that integration was studied using cells depleted of SecDF rather than SecE/Y (72). Furthermore, F_ob integration was examined using a F_ob variant with an N-terminal T7 tag, which may affect the biogenesis requirements of F_ob.

Our analysis of the inner membrane proteome of SecE-depleted and control cells allowed us to search for common features among proteins whose levels were reduced, unaffected, or increased in the membrane of SecE-depleted cells. Our observations could be explained by differences in access to the remaining Sec translocons. However, we found no correlations between the effect of SecE depletion and the properties of the first transmembrane segment (e.g., hydrophobicity), as could be expected if the differences were due to different affinities toward the residual translocons. Interestingly, we did find that the inner membrane proteins whose levels were either unaffected or increased upon depletion of SecE do lack large periplasmic domains and/or consist of only one or two transmembrane segments (Fig. 7; see Table S5 in the supplemental material). Notably, all the proteins that so far have been shown to integrate via the Sec translocon-independent, YidC-dependent pathway (M13, Pf3, F_oc, a tandem F_oc construct, MscL and a C-terminally truncated ProW variant) have similar features (34, 64). Thus, it is tempting to speculate that the proteins whose levels are unaffected or increased in the membrane of SecE-depleted cells are potential substrates of the YidC-only pathway. Recently, it was shown that insertion of two proteins was unaffected by either SecE or YidC depletion. One of these proteins was KdpD, which consists of four transmembrane segments, short periplasmic loops, and exceptionally large cytoplasmic N- and C-terminal domains, and the other was a Pf3-H1Lep-P2 hybrid construct, which consists of the short N-terminal periplasmic loop from the Pf3 coat protein, the first transmembrane segment, and the large cytoplasmic P2 domain of Lep (22, 64). Thus, both KdpD and Pf3-H1Lep-P2 have the features that we found to be overrepresented among the inner membrane proteins that appeared to be unaffected by the depletion of SecE. It is also possible that some integral membrane proteins, just like some secretory proteins, are promiscuous; i.e., they use the insertion pathway that is available.

Clearly, the observation that the levels of such a large number of inner membrane proteins appear to be unaffected or increased upon SecE depletion is intriguing and warrants further investigation. For instance, it would be interesting to study these proteins individually using pulse-labeling-based targeting and assembly assays (25). In addition, we are currently analyzing membrane protein biogenesis in a YidC depletion strain using a proteomics approach similar to the one used here.

In conclusion, substantial protein translocation and insertion activity was still observed in SecE-depleted cells. This suggests that the significance of Sec translocon-independent translocation/insertion and pathway promiscuity in outer and inner membrane protein biogenesis have been underestimated. Our study provides several testable hypotheses and new substrates that can be used to further determine guiding principles for protein translocation and insertion in the model organism *E. coli*.

ACKNOWLEDGMENTS

Claudia Wagner is thanked for assistance with the flow cytometry experiments. Dirk-Jan Scheffers and Joen Luirink are thanked for critically reading the manuscript.

This research was supported by grants from the Swedish Research Council, the Carl Tryggers Stiftelse, the Marianne and Marcus Wallenberg Foundation, and the SSF-supported Center for Biomembrane Research to J.W.D.G. and by a grant from The Swedish Foundation for International Cooperation in Research and Higher Education (STINT) to J.W.D.G. and K.J.V.W. Proteomics infrastructure was supported by a grant from NYSTAR to K.J.V.W.

REFERENCES

1. **Akiyama, Y., A. Kihara, H. Tokuda, and K. Ito.** 1996. FtsH (HflB) is an ATP-dependent protease selectively acting on SecY and some other membrane proteins. J. Biol. Chem. **271:**31196–31201.
2. **Alami, M., K. Dalal, B. Lelj-Garolla, S. G. Sligar, and F. Duong.** 2007. Nanodiscs unravel the interaction between the SecYEG channel and its cytosolic partner SecA. EMBO J. **26:**1995–2004.
3. **Andersson, H., and G. von Heijne.** 1993. Sec dependent and Sec independent

assembly of E. coli inner membrane proteins: the topological rules depend on chain length. EMBO J. **12:**683–691.
4. **Arsene, F., T. Tomoyasu, and B. Bukau.** 2000. The heat shock response of Escherichia coli. Int. J. Food Microbiol. **55:**3–9.
5. **Baars, L., A. J. Ytterberg, D. Drew, S. Wagner, C. Thilo, K. J. van Wijk, and J. W. de Gier.** 2006. Defining the role of the Escherichia coli chaperone SecB using comparative proteomics. J. Biol. Chem. **281:**10024–10034.
6. **Baba, T., T. Ara, M. Hasegawa, Y. Takai, Y. Okumura, M. Baba, K. A. Datsenko, M. Tomita, B. L. Wanner, and H. Mori.** 2006. Construction of Escherichia coli K-12 in-frame, single-gene knockout mutants: the Keio collection. Mol. Syst. Biol. **2:**2006.0008.
7. **Berven, F. S., O. A. Karlsen, J. C. Murrell, and H. B. Jensen.** 2003. Multiple polypeptide forms observed in two-dimensional gels of Methylococcus capsulatus (Bath) polypeptides are generated during the separation procedure. Electrophoresis **24:**757–761.
8. **Bessonneau, P., V. Besson, I. Collinson, and F. Duong.** 2002. The SecYEG preprotein translocation channel is a conformationally dynamic and dimeric structure. EMBO J. **21:**995–1003.
9. **Blattner, F. R., G. Plunkett, C. A. Bloch, N. T. Perna, V. Burland, M. Riley, J. Collado-Vides, J. D. Glasner, C. K. Rode, G. F. Mayhew, J. Gregor, N. W. Davis, H. A. Kirkpatrick, M. A. Goeden, D. J. Rose, B. Mau, and Y. Shao.** 1997. The complete genome sequence of Escherichia coli K-12. Science **277:**1453–1462.
10. **Carrio, M. M., and A. Villaverde.** 2005. Localization of chaperones DnaK and GroEL in bacterial inclusion bodies. J. Bacteriol. **187:**3599–3601.
11. **Carrio, M. M., and A. Villaverde.** 2003. Role of molecular chaperones in inclusion body formation. FEBS Lett. **537:**215–221.
12. **Celebi, N., L. Yi, S. J. Facey, A. Kuhn, and R. E. Dalbey.** 2006. Membrane biogenesis of subunit II of cytochrome bo oxidase: contrasting requirements for insertion of N-terminal and C-terminal domains. J. Mol. Biol. **357:**1428–1436.
13. **Chen, Y., P. C. Tai, and S. F. Sui.** 2007. The active ring-like structure of SecA revealed by electron crystallography: conformational change upon interaction with SecB. J. Struct. Biol. **159:**149–153.
14. **Choy, J. S., L. L. Aung, and A. W. Karzai.** 2007. Lon protease degrades transfer-messenger RNA-tagged proteins. J. Bacteriol. **189:**6564–6571.
15. **Cristobal, S., P. Scotti, J. Luirink, G. von Heijne, and J. W. L. de Gier.** 1999. The signal recognition particle-targeting pathway does not necessarily deliver proteins to the Sec-translocase in Escherichia coli. J. Biol. Chem. **274**:20068–20070.
16. **Dalbey, R. E., and M. Chen.** 2004. Sec-translocase mediated membrane protein biogenesis. Biochim. Biophys. Acta **1694:**37–53.
17. **Daley, D. O., M. Rapp, E. Granseth, K. Melen, D. Drew, and G. von Heijne.** 2005. Global topology analysis of the Escherichia coli inner membrane proteome. Science **308:**1321–1323.
18. **Darwin, A. J.** 2005. The phage-shock-protein response. Mol. Microbiol. **57:**621–628.
19. **Driessen, A. J. M., E. H. Manting, and C. van der Does.** 2001. The structural basis of protein targeting and translocation in bacteria. Nat. Struct. Biol. **8:**492–498.
20. **du Plessis, D. J., N. Nouwen, and A. J. Driessen.** 2006. Subunit a of cytochrome o oxidase requires both YidC and SecYEG for membrane insertion. J. Biol. Chem. **281:**12248–12252.
21. **Facey, S. J., and A. Kuhn.** 2004. Membrane integration of E. coli model membrane proteins. Biochim. Biophys. Acta **1694:**55–66.
22. **Facey, S. J., and A. Kuhn.** 2003. The sensor protein KdpD inserts into the Escherichia coli membrane independent of the Sec translocase and YidC. Eur. J. Biochem. **270:**1724–1734.
23. **Fernandez-Escamilla, A. M., F. Rousseau, J. Schymkowitz, and L. Serrano.** 2004. Prediction of sequence-dependent and mutational effects on the aggregation of peptides and proteins. Nat. Biotechnol. **22:**1302–1306.
24. **Fishov, I., and C. L. Woldringh.** 1999. Visualization of membrane domains in Escherichia coli. Mol. Microbiol. **32:**1166–1172.
25. **Froderberg, L., E. Houben, J. C. Samuelson, M. Y. Chen, S. K. Park, G. J. Phillips, R. Dalbey, J. Luirink, and J. W. L. de Gier.** 2003. Versatility of inner membrane protein biogenesis in Escherichia coli. Mol. Microbiol. **47:**1015–1027.
26. **Froderberg, L., T. Rohl, K. J. van Wijk, and J. W. de Gier.** 2001. Complementation of bacterial SecE by a chloroplastic homologue. FEBS Lett. **498**: 52–56.
27. **Gittins, J. R., D. A. Phoenix, and J. M. Pratt.** 1994. Multiple mechanisms of membrane anchoring of Escherichia coli penicillin-binding proteins. FEMS Microbiol. Rev. **13:**1–12.
28. **Hatzixanthis, K., T. Palmer, and F. Sargent.** 2003. A subset of bacterial inner membrane proteins integrated by the twin-arginine translocase. Mol. Microbiol. **49:**1377–1390.
29. **Herskovits, A. A., E. Shimoni, A. Minsky, and E. Bibi.** 2002. Accumulation of endoplasmic membranes and novel membrane-bound ribosome-signal recognition particle receptor complexes in Escherichia coli. J. Cell Biol. **159:**403–410.
30. **Hessa, T., H. Kim, K. Bihlmaier, C. Lundin, J. Boekel, H. Andersson, I. Nilsson, S. H. White, and G. von Heijne.** 2005. Recognition of transmembrane helices by the endoplasmic reticulum translocon. Nature **433:**377–381.
31. **Hewitt, C. J., and G. Nebe-Von-Caron.** 2004. The application of multi-parameter flow cytometry to monitor individual microbial cell physiological state. Adv. Biochem. Eng. Biotechnol. **89:**197–223.
32. **Ito, K., and Y. Akiyama.** 2005. Cellular functions, mechanism of action, and regulation of FtsH protease. Annu. Rev. Microbiol. **59:**211–231.
33. **Kang, S. W., N. S. Rane, S. J. Kim, J. L. Garrison, J. Taunton, and R. S. Hegde.** 2006. Substrate-specific translocational attenuation during ER stress defines a pre-emptive quality control pathway. Cell **127:**999–1013.
34. **Kiefer, D., and A. Kuhn.** 2007. YidC as an essential and multifunctional component in membrane protein assembly. Int. Rev. Cytol **259:**113–138.
35. **Laskowska, E., J. Bohdanowicz, D. Kuczynska-Wisnik, E. Matuszewska, S. Kedzierska, and A. Taylor.** 2004. Aggregation of heat-shock-denatured, endogenous proteins and distribution of the IbpA/B and Fda marker-proteins in Escherichia coli WT and grpE280 cells. Microbiology **150:**247–259.
36. **Lee, P. A., D. Tullman-Ercek, and G. Georgiou.** 2006. The bacterial twin-arginine translocation pathway. Annu. Rev. Microbiol. **60:**373–395.
37. **Luirink, J., G. von Heijne, E. Houben, and J. W. de Gier.** 2005. Biogenesis of inner membrane proteins in Escherichia coli. Annu. Rev. Microbiol. **59:**329–355.
38. **Manting, E. H., and A. J. Driessen.** 2000. Escherichia coli translocase: the unravelling of a molecular machine. Mol. Microbiol. **37:**226–238.
39. **Marani, P., S. Wagner, L. Baars, P. Genevaux, J. W. de Gier, I. Nilsson, R. Casadio, and G. von Heijne.** 2006. New Escherichia coli outer membrane proteins identified through prediction and experimental verification. Protein Sci. **15:**884–889.
40. **Mitra, K., J. Frank, and A. Driessen.** 2006. Co- and post-translational translocation through the protein-conducting channel: analogous mechanisms at work? Nat. Struct. Mol. Biol. **13:**957–964.
41. **Mitra, K., C. Schaffitzel, T. Shaikh, F. Tama, S. Jenni, C. L. Brooks III, N. Ban, and J. Frank.** 2005. Structure of the E. coli protein-conducting channel bound to a translating ribosome. Nature **438:**318–324.
42. **Mogk, A., C. Schlieker, K. L. Friedrich, H. J. Schonfeld, E. Vierling, and B. Bukau.** 2003. Refolding of substrates bound to small Hsps relies on a disaggregation reaction mediated most efficiently by ClpB/DnaK. J. Biol. Chem. **278:**31033–31042.
43. **Molloy, M. P., B. R. Herbert, M. B. Slade, T. Rabilloud, A. S. Nouwens, K. L. Williams, and A. A. Gooley.** 2000. Proteomic analysis of the Escherichia coli outer membrane. Eur. J. Biochem. **267:**2871–2881.
44. **Nakatogawa, H., A. Murakami, and K. Ito.** 2004. Control of SecA and SecM translation by protein secretion. Curr. Opin. Microbiol. **7:**145–150.
45. **Neuhoff, V., N. Arold, D. Taube, and W. Ehrhardt.** 1988. Improved staining of proteins in polyacrylamide gels including isoelectric focusing gels with clear background at nanogram sensitivity using Coomassie brilliant blue G-250 and R-250. Electrophoresis **9:**255–262.
46. **Nouwen, N., and A. J. Driessen.** 2002. SecDFyajC forms a heterotetrameric complex with YidC. Mol. Microbiol. **44:**1397–1405.
47. **Oakley, B. R., D. R. Kirsch, and N. R. Morris.** 1980. A simplified ultrasensitive silver stain for detecting proteins in polyacrylamide gels. Anal. Biochem. **105:**361–363.
48. **Osborne, A. R., and T. A. Rapoport.** 2007. Protein translocation is mediated by oligomers of the SecY complex with one SecY copy forming the channel. Cell **129:**97–110.
49. **Osborne, A. R., T. A. Rapoport, and B. van den Berg.** 2005. Protein translocation by the Sec61/SecY channel. Annu. Rev. Cell Dev. Biol. **21:**529–550.
50. **Peltier, J. B., O. Emanuelsson, D. E. Kalume, J. Ytterberg, G. Friso, A. Rudella, D. A. Liberles, L. Soderberg, P. Roepstorff, G. von Heijne, and K. J. van Wijk.** 2002. Central functions of the lumenal and peripheral thylakoid proteome of Arabidopsis determined by experimentation and genome-wide prediction. Plant Cell **14:**211–236.
51. **Peltier, J. B., A. J. Ytterberg, Q. Sun, and K. J. van Wijk.** 2004. New functions of the thylakoid membrane proteome of Arabidopsis thaliana revealed by a simple, fast, and versatile fractionation strategy. J. Biol. Chem. **279:**49367–49383.
52. **Qi, H. Y., J. B. Hyndman, and H. D. Bernstein.** 2002. DnaK promotes the selective export of outer membrane protein precursors in SecA-deficient Escherichia coli. J. Biol. Chem. **277:**51077–51083.
53. **Randall, L. L., and S. J. Hardy.** 2002. SecB, one small chaperone in the complex milieu of the cell. Cell. Mol. Life Sci. **59:**1617–1623.
54. **Rey, S., M. Acab, J. L. Gardy, M. R. Laird, K. deFays, C. Lambert, and F. S. Brinkman.** 2005. PSORTdb: a protein subcellular localization database for bacteria. Nucleic Acids Res. **33:**D164—D168.
55. **Rosen, R., and E. Z. Ron.** 2002. Proteome analysis in the study of the bacterial heat-shock response. Mass Spectrom. Rev. **21:**244–265.
56. **Ruiz, N., D. Kahne, and T. J. Silhavy.** 2006. Advances in understanding bacterial outer-membrane biogenesis. Nat. Rev. Microbiol. **4:**57–66.
57. **Ruiz, N., and T. J. Silhavy.** 2005. Sensing external stress: watchdogs of the Escherichia coli cell envelope. Curr. Opin. Microbiol. **8:**122–126.
58. **Schagger, H., and G. von Jagow.** 1991. Blue native electrophoresis for isolation of membrane protein complexes in enzymatically active form. Anal. Biochem. **199:**223–231.

59. **Tomoyasu, T., A. Mogk, H. Langen, P. Goloubinoff, and B. Bukau.** 2001. Genetic dissection of the roles of chaperones and proteases in protein folding and degradation in the Escherichia coli cytosol. Mol. Microbiol. **40:**397–413.
60. **Traxler, B., and C. Murphy.** 1996. Insertion of the polytopic membrane protein MalF is dependent on the bacterial secretion machinery. J. Biol. Chem. **271:**12394–12400.
61. **Tullman-Ercek, D., M. P. DeLisa, Y. Kawarasaki, P. Iranpour, B. Ribnicky, T. Palmer, and G. Georgiou.** 2007. Export pathway selectivity of Escherichia coli twin arginine translocation signal peptides. J. Biol. Chem. **282:**8309–8316.
62. **van Bloois, E., G. J. Haan, J. W. de Gier, B. Oudega, and J. Luirink.** 2006. Distinct requirements for translocation of the N-tail and C-tail of the Escherichia coli inner membrane protein CyoA. J. Biol. Chem. **281:**10002–10009.
63. **van Bloois, E., G. Jan Haan, J. W. de Gier, B. Oudega, and J. Luirink.** 2004. $F_{(1)}F_{(0)}$ ATP synthase subunit c is targeted by the SRP to YidC in the E. coli inner membrane. FEBS Lett. **576:**97–100.
64. **van Bloois, E., C. M. Ten Hagen-Jongman, and J. Luirink.** 2007. Flexibility in targeting and insertion during bacterial membrane protein biogenesis. Biochem. Biophys. Res. Commun. **362:**727–733.
65. **Van den Berg, B., W. M. Clemons, Jr., I. Collinson, Y. Modis, E. Hartmann, S. C. Harrison, and T. A. Rapoport.** 2004. X-ray structure of a protein-conducting channel. Nature **427:**36–44.
66. **van der Laan, M., P. Bechtluft, S. Kol, N. Nouwen, and A. J. Driessen.** 2004. F_1F_0 ATP synthase subunit c is a substrate of the novel YidC pathway for membrane protein biogenesis. J. Cell Biol. **165:**213–222.
67. **Wagner, S., L. Baars, A. J. Ytterberg, A. Klussmeier, C. S. Wagner, O. Nord, P. A. Nygren, K. J. van Wijk, and J. W. de Gier.** 2007. Consequences of membrane protein overexpression in Escherichia coli. Mol. Cell. Proteomics **9:**1527–1550.
68. **Weibezahn, J., P. Tessarz, C. Schlieker, R. Zahn, Z. Maglica, S. Lee, H. Zentgraf, E. U. Weber-Ban, D. A. Dougan, F. T. Tsai, A. Mogk, and B. Bukau.** 2004. Thermotolerance requires refolding of aggregated proteins by substrate translocation through the central pore of ClpB. Cell **119:**653–665.
69. **Withey, J. H., and D. I. Friedman.** 2003. A salvage pathway for protein structures: tmRNA and trans-translation. Annu. Rev. Microbiol. **57:**101–123.
70. **Wu, C. C., and J. R. Yates.** 2003. The application of mass spectrometry to membrane proteomics. Nat. Biotechnol. **21:**262–267.
71. **Xie, K., D. Kiefer, G. Nagler, R. E. Dalbey, and A. Kuhn.** 2006. Different regions of the nonconserved large periplasmic domain of Escherichia coli YidC are involved in the SecF interaction and membrane insertase activity. Biochemistry **45:**13401–13408.
72. **Yi, L., N. Celebi, M. Chen, and R. E. Dalbey.** 2004. Sec/SRP requirements and energetics of membrane insertion of subunits a, b, and c of the Escherichia coli F_1F_0 ATP synthase. J. Biol. Chem. **279:**39260–39267.
73. **Zabrouskov, V., X. Han, E. Welker, H. Zhai, C. Lin, K. J. van Wijk, H. A. Scheraga, and F. W. McLafferty.** 2006. Stepwise deamidation of ribonuclease A at five sites determined by top down mass spectrometry. Biochemistry **45:**987–992.